Recursive tiling and geometry of piecewise rotations by $\pi/7$

J.H.Lowenstein*, K.L.Kouptsov*, F. Vivaldi†

*Dept. of Physics, New York University, 2 Washington Place,
New York, NY 10003, USA
†School of Mathematical Sciences, Queen Mary, University of London,
London E1 4NS, UK

Abstract

We study two piecewise affine maps on convex polygons, locally conjugate to a rotation by a multiple of $\pi/7$. We obtain a finite-order recursive tiling of the phase space by return map sub-domains of triangles and periodic heptagonal domains (cells), with scaling factors given by algebraic units. This tiling allows one efficiently to construct periodic orbits of arbitrary period, and to obtain a convergent sequence of coverings of the closure $\overline{\Gamma}$ of the discontinuity set Γ. For every map for which such finite-order recursive tiling exists, we derive sufficient conditions for the equality of Hausdorff and box-counting dimensions, and for the existence of a finite, non-zero Hausdorff measure of $\overline{\Gamma}$. We then verify that these conditions apply to our models, we obtain an irreducible transcendental equation for the Hausdorff dimension involving fundamental units, and establish the existence of infinitely many disjoint invariant components of the residual set $\overline{\Gamma} \setminus \Gamma$. We calculate numerically the asymptotic power law growth of the number of cells as a function of maximum return time, as well as the number of cells of diameter larger than a specified ϵ. In the latter case, the exponent is shown to coincide with the Hausdorff dimension.

1 Introduction

There has been a great deal of interest recently in piecewise isometries of convex polygons and polyhedra. These are usually implemented as piecewise affine maps, consisting of a linear part linearly conjugate to a rotation (which we still call a rotation), followed by a translation. These dynamical systems, important in theory and applications, derive their remarkably complex behaviour from discontinuity rather than nonlinearity. Their description presents considerable difficulties, and requires the development of new mathematical and computational tools. Piecewise isometries have appeared in the study of polygonal dual billiards [23, 37–39, 41], polygonal exchange transformations [7, 15–21, 24], kicked oscillators and saw-tooth Hamiltonian dynamics [3, 26], and are of intrinsic interest in ergodic theory [1, 8, 26, 27]. Applications include digital filters with overflow nonlinearity [4, 9–11, 13, 42], round-off errors in linear systems [29, 31–33, 40], impact oscillators [6].

A central object of study in a piecewise isometry is the *discontinuity set* Γ (the set of points which eventually experience the discontinuity), which is constructed recursively as the set of pre-images of the points where the map itself is discontinuous. Of equal importance are the *cells*, convex polyhedra of maximal dimension, which are periodic under the mapping. The two sets are closely related: the complement of the set of all cells, the *exceptional set*, is the closure of the discontinuity set. Finally, we have the so-called *residual set* Σ, which is the complement of the discontinuity set in its closure: $\Sigma = \overline{\Gamma} \setminus \Gamma$.

An exhaustive treatment has been given, by several authors, for specific models of piecewise affine mappings of convex polygons. In these models, the linear part is conjugated to a rotation by the angle $2\pi p/q$, with trace $\lambda = 2\cos 2\pi p/q$, a *quadratic irrational* (root of a quadratic polynomial with integer coefficients). Although many general questions remain open, for these models one has obtained (i) a systematic construction of all cells, and consequent proof that they exhaust the measure; (ii) fractal structure and dynamics of Γ. Some of these results rely crucially on computer-assisted proofs, which exploit the discrete nature of the dynamics [29]. The main dynamical objects are effectively described by restricting coordinates to the field $\mathbf{Q}(\lambda)$, the set obtained by adjoining λ to the rationals. Because λ is a root of a polynomial with integer coefficients, in computations it is treated symbolically, except when it appears in an inequality, in which case it is sandwiched between good rational approximants. In all cases, computations are exact.

The key to the analysis of these models is the existence of a *finite number* of triangular *scaling domains,* each containing an infinite sequence of similar domains converging to a point on the boundary. The first-return map of each domain in the sequence is a rescaled version of the first-return map at the top level, and scaling constants are given by *units* (invertible elements) in the respective rings of algebraic integers. Within the domain sequences one finds a finite number of cell sequences which exhaust the set of all cells, apart from finitely many exceptions. These results echo that obtained by Boshernitzan and Carrol [5] on interval exchange transformations defined by quadratic irrationals, which were shown to feature finitely many transformations up to rescaling. For 2-interval exchange, this finiteness result reduces to Lagrange's theorem on the eventual periodicity of the continued fractions expansions of quadratic surds.

Scaling domains also have the property of *recursive tiling,* whereby each domain in a scaling sequence is covered by a finite set of images of a rescaled copy of itself, plus a finite number of periodic cells. The former amounts to a nested sequence of *finite coverings* of the residual set, which allows one to obtain exact information on its geometrical and dynamical properties.

There is now a great deal of interest in extending the results for two-dimensional maps with quadratic parameter λ, to more general piecewise isometries in two and higher dimensions. An attempt was made to apply the method of recursive return-map partitions to 4-dimensional examples with cubic λ, but the results were inconclusive, and highlighted great computational difficulties [33]. More promising are recent investigations of two-dimensional maps with rotation angle $\pi/7$ (cubic λ) acting on triangles and rhombi [22, 28]. One has been able to establish the existence of domains with unbounded return time, prove the existence of infinitely many probability measures on symbol space, bound the Hausdorff dimension of the discontinuity set, and provide considerable evidence for self-similarity in the return map partition.

In this paper we concentrate on the analysis of the periodic cells and the residual set for two mappings with cubic λ (rotation by $\pi/7$) acting on a triangle and a square, respectively. The results include theorems proved with computer assistance, as well as high-precision numerical calculations based on those theorems. The key ingredient in our analysis is the construction of a *recursive tiling* of domains, which requires generalizing the notion of scaling domain. Instead of tiling a domain (up to finitely many cells) by the return-map orbit of a rescaled copy of itself, we tile it by the orbits of finitely many domains, each equivalent (under a certain group of transformations) to a member of a *finite catalogue* of domain prototypes. Each of the sub-domains is similarly tiled, using the same catalogue. This scheme provides a finite-order recursive algorithm for generating all cells, as well as a nested sequence of finite coverings of the residual set, which affords the computation of dimensions and period asymptotics, and which circumvents the difficulty of unbounded return time to a domain.

The mathematical machinery of finite-order recursive tiling will be set forth in Section 2 below, and then applied in Section 3, to two models sharing the same rotational part, but acting on different domains. We consider a triangular domain with a tripartite return map, and a more complicated map of a square domain, introduced to illustrate a more typical level of complexity. For these models we prove, with computer assistance, the existence of finite-order recursive tiling with scaling factors given by algebraic units (theorems 2 and 3). For reason of space, the details of the computer-assisted proofs are provided only in electronic form, as Mathematica notebooks [34]. In the example of the square, because the catalogue is quite large and the tilings more elaborate, also the defining parameters of the system are largely relegated to electronic form. Ascertaining how generic is the finite-order property established in our two examples is an important open problem.

In Section 4, we provide a sufficient condition for the equality of Hausdorff and box-counting dimensions and the existence of a finite, non-zero Hausdorff measure for the exceptional set of a domain with finite-order recursive tiling (Theorem 4). Under the same conditions, we also construct a closely related invariant measure for the residual set (Corollary 5). For the examples considered, we then verify the hypothesis of the theorem, and derive a transcendental equation for the dimension, which can be computed to any convenient precision. Finally, we show that the nontrivial invariant measure for the tiles extends to infinitely many disjoint invariant subsets of the residual set Σ, thus establishing the existence of infinitely many disjoint invariant components.

Section 5 will be devoted to an efficient numerical algorithm, based on recursive tiling, to calculate the growth in the number of periodic orbits as a function of first return time. We find an asymptotic power law and calculate the power to four significant digits. A similar technique is used to calculate the growth in the number of cells of diameter greater than ϵ, for ϵ tending to zero. The asymptotic power can be shown to be precisely the Hausdorff dimension, and our numerical calculation is consistent with this to four significant digits.

The tables of data are collected in Section 6.

We are grateful to A. Goetz and B. Kahng for useful discussions, and to A. Goetz and G. Poggiaspalla for making available to us an early version of Ref. [22]. The useful remarks of one referee helped us improve the correctness and clarity of the paper, particularly in Section 4.

2 Preliminaries and definitions

We begin with a map C on $\mathbf{R}^2$ linearly conjugate to a rotation with rational rotation number p/q

$$\zeta \mapsto C \cdot \zeta \qquad \zeta = \begin{pmatrix} \zeta_0 \\ \zeta_1 \end{pmatrix} \qquad C^q = 1.$$

The trace λ of C is given by

$$\lambda = \mathrm{Tr}(C) = 2 \cos \frac{2\pi p}{q}$$

and the eigenvalues of C satisfy the polynomial equation $x^q - 1 = 0$. From this it is not difficult to show that λ is also a root of a polynomial with integer coefficients and unit leading coefficient, namely λ is an *algebraic integer.* If n is the degree of this polynomial[1], then we define the algebraic number ring

$$\mathbf{Z}[\lambda] = \left\{ k_0 + k_1 \lambda + \cdots + k_{n-1} \lambda^{n-1} \ : \ k_i \in \mathbf{Z} \right\}$$

which is the collection of all algebraic integers in the field $\mathbf{Q}(\lambda)$ [2, p. 48]. The field $\mathbf{Q}(\lambda)$ is the subset of $\mathbf{R}$ obtained by letting $k_i \in \mathbf{Q}$ in the above expression.

It is expedient to require that all entries of C belong to $\mathbf{Z}[\lambda]$, which ensures that the action of C does not increase the size of denominators in the coordinate field. A common choice for such matrix is

$$C = \begin{pmatrix} 0 & 1 \\ -1 & \lambda \end{pmatrix}$$

which is the matrix considered in this paper. We select the rotation number $p/q = 1/14$, corresponding to a cubic field ($n = 3$):

$$\lambda^3 - \lambda^2 - 2\lambda + 1 = 0 \qquad \lambda = 2\cos\frac{\pi}{7} = 1.8019... \tag{1}$$

Of importance will be the units in $\mathbf{Z}[\lambda]$, namely those $\eta \in \mathbf{Z}[\lambda]$ such that $\eta^{-1} \in \mathbf{Z}[\lambda]$. The units form a finitely generated multiplicative group. In particular, From Dirichlet's unit theorem [12, page 210], any positive unit η in a real cubic field can be written in the form

$$\eta = \eta_1^{m_1} \eta_2^{m_2}$$

where m_1 and m_2 are integers, and η_1 and η_2 are two *fundamental units.* The choice of fundamental units is non-unique; for definiteness, for $p/q = 1/14$ we shall use [12, appendix B.3]

$$\eta_1 = 2 + \lambda - \lambda^2 = \lambda^{-1}, \qquad \eta_2 = -1 - \lambda + \lambda^2 = (-1 + \lambda^2)^{-1} = 1 - \eta_1. \tag{2}$$

Note that here λ itself is a unit, which is not true for general rotation numbers.

We are interested in cases where an open convex polygon $\mathcal{D}$ is partitioned (apart from a set of dimension 1) into a finite number of open convex polygons $\mathcal{D}_i$, on each of which there is an affine map

$$\rho_i : \zeta \mapsto C^{\nu_i} \zeta + \delta_i, \qquad \delta_i \in \mathbf{Z}[\lambda]^2$$

[1] One has $n = \phi(q)/2$, where ϕ is Euler's totient function [2]

such that

$$\rho_i \mathcal{D}_i \subset \mathcal{D}, \qquad \overline{\bigcup_i \rho_i \mathcal{D}_i} = \overline{\mathcal{D}},$$

where the overline denotes closure. The polygon $\mathcal{D}$ is assumed to be bounded by lines oriented along a subset of the q basis vectors $u^{(m)}$, with

$$u^{(0)} = \begin{pmatrix} 1 \\ 0 \end{pmatrix}, \qquad u^{(m)} = C' u^{(m-1)} \qquad m = 0, \dots, q-1$$

where C' is the transpose of matrix C.

We define a **domain** to be a convex polygon with each bounding line satisfying an equation of the form

$$u^{(m)} \cdot \zeta = b \qquad b \in \mathbf{Z}[\lambda]. \tag{3}$$

We use the notation $\mathcal{D}(\mathbf{m}, \mathbf{s}, \mathbf{b})$ to specify a domain with K sides, with

$$\begin{array}{rclll} \mathbf{m} & = & (m_0, \dots, m_{K-1}) & & m_k \in \{0, \dots, q-1\} \\ \mathbf{s} & = & (s_0, \dots, s_{K-1}) & & s_k \in \{-1, 1\} \\ \mathbf{b} & = & (b_0, \dots, b_{K-1}) & & b_k \in \mathbf{Z}[\lambda], \end{array} \tag{4}$$

where each triple (m_k, s_k, b_k) corresponds to the bound

$$u^{(m_k)} \cdot \zeta \begin{cases} < b_k, & s_k = 1 \\ \geq b_k, & s_k = -1. \end{cases} \tag{5}$$

The value of s_k determines the nature of the bound (upper or lower); when q is even, $u^{(m)} = -u^{(m+q/2 \,(\mathrm{mod}\; q))}$, and one can list the bounds of an open domain with all $s_k = 1$.

We introduce a group $\mathcal{G}$ of operators acting on domains. This group is generated by a (generalized) rotation C, a reflection R, translation by a vector T_δ, and rescaling by a factor S_ω, and it acts as follows

$$\begin{array}{rcll} C\mathcal{D}(\mathbf{m}, \mathbf{s}, \mathbf{b}) & = & \mathcal{D}(\mathbf{m}', \mathbf{s}, \mathbf{b}) & m'_k \equiv m_k - 1 \,(\mathrm{mod}\; q) \\ R\mathcal{D}(\mathbf{m}, \mathbf{s}, \mathbf{b}) & = & \mathcal{D}(\tilde{\mathbf{m}}, \mathbf{s}, \mathbf{b}) & \tilde{m}_k = \begin{cases} q/2 - 1 - m_k, & 0 \leq m_k < q/2 \\ 3q/2 - 1 - m_k, & q/2 \leq m_k < q \end{cases} \qquad (q \text{ even}) \\ T_\delta \mathcal{D}(\mathbf{m}, \mathbf{s}, \mathbf{b}) & = & \mathcal{D}(\mathbf{m}, \mathbf{s}, \mathbf{b}') & \delta \in \mathbf{Z}^2[\lambda], \quad b'_k = b_k + u^{(k)} \cdot \delta \\ S_\omega \mathcal{D}(\mathbf{m}, \mathbf{s}, \mathbf{b}) & = & \mathcal{D}(\mathbf{m}, \mathbf{s}, \omega \mathbf{b}) & \omega \in \mathbf{Q}(\lambda). \end{array}$$

For $p/q = 1/14$, the above operators correspond to the following point-wise actions on $\zeta = (\zeta_0, \zeta_1)$

$$\begin{array}{rcl} C\zeta & = & (\zeta_1, \lambda\zeta_1 - \zeta_0) \\ R\zeta & = & (\zeta_1 - \lambda\zeta_0, \lambda\zeta_1 + (1 - \lambda^2)\zeta_0) \\ T_\delta \zeta & = & (\zeta_0 + \delta_0, \zeta_1 + \delta_1) \\ S_\omega \zeta & = & (\omega\zeta_0, \omega\zeta_1). \end{array}$$

These operators have the following product and commutation properties

$$T_\delta \circ T_\epsilon = T_{\delta+\epsilon} \qquad S_\omega \circ S'_\omega = S_{\omega\omega'} \qquad R^2 = 1$$

$$S_\omega \circ C = C \circ S_\omega \qquad S_\omega \circ R = R \circ S_\omega \qquad R \circ C = C^{-1} \circ R$$

$$g \circ T_\delta = T_{g\delta} \circ g, \quad g \in \{C, R, S_\omega\}$$

using which we can write any element g of $\mathcal{G}$ in the form

$$g(\kappa, \nu, \delta, \omega) = S_\omega \circ T_\delta \circ C^\nu \circ R^\kappa. \tag{6}$$

In what follows, we shall be interested in domains equipped with a piecewise affine dynamics. These, in turn, have sub-domains, with piecewise affine dynamics induced by the first return map of the parent domain. The following definitions make these notions precise

Let $\mathcal{D}$ be a domain. A mapping $\rho : \mathcal{D} \to \mathcal{D}$ is a **domain map** for $\mathcal{D}$, if $\mathcal{D}$ is partitioned (up to a set of measure zero) into a finite number of open sub-domains $\mathcal{D}_j$, such that the restriction ρ_j of ρ to $\mathcal{D}_j$ takes the form $\rho_j = T_{\delta_j} \circ C^{\nu_j}$, where $\delta_j \in \mathbf{Z}[\lambda]^2$ and ν_j is a non-negative integer.

A **dressed domain** is a pair $\Delta = (\mathcal{D}, \rho)$, where $\mathcal{D}$ is a domain and ρ is a domain map for $\mathcal{D}$. A **dressed sub-domain** $\Delta' = (\mathcal{D}', \rho')$ of a dressed domain $\Delta = (\mathcal{D}, \rho)$ is a dressed domain such that $\mathcal{D}' \subset \mathcal{D}$ and ρ' is the first-return map on $\mathcal{D}'$ induced by ρ. The **return orbit** (with respect to ρ) of Δ' is the finite union of disjoint orbits

$$\mathcal{U}' = \bigcup_j \left\{ \rho^s \mathcal{D}'_j \,:\, s = 0, \ldots, t'_j - 1' \right\},$$

where $\mathcal{D}'_j$ is the jth tile of $\mathcal{D}'$, and t'_j is the first-return time of $\mathcal{D}'_j$ with respect to ρ.

In what follows, an important role will be played by the periodic sub-domains Π —or **cells**— of a dressed domain $\Delta = (\mathcal{D}, \rho)$, and their **return orbits** (with respect to ρ), given by

$$\mathcal{P} = \{\rho^s \Pi \,:\, s = 0, \ldots, t - 1\}$$

where t is the minimal period of Π.

We speak of a **partition** of a domain $\mathcal{D}$ by a finite set of disjoint sub-domains $\mathcal{D}^{(i)}$ if the closure of $\mathcal{D}$ is equal to the union of the closures of the $\mathcal{D}^{(i)}$.

The above definitions apply to general rotation numbers p/q, provided that the parameters defining a domain map —the bounds b defining a domain (Equation (3)) and the components of the translation vectors δ_i— are allowed to range in the module $\mathbf{Z}[\lambda]/a$, where a is a positive integer determined uniformly [29]. Here $a = 1$.

Next we define the action of $\mathcal{G}$ on dressed domains as follows

$$g\,\Delta \stackrel{\text{def}}{=} (g\mathcal{D},\, g\rho g^{-1}) \qquad \Delta = (\mathcal{D}, \rho), \qquad g \in \mathcal{G}. \tag{7}$$

One verifies that $g\Delta$ is a dressed domain, and that (7) is indeed a group action. Such action induces an equivalence relation on dressed domains, the equivalence classes being the orbits of $\mathcal{G}$. In other words, two dressed domains Δ and Δ' are **equivalent** (w.r.t $\mathcal{G}$, written $\Delta \sim \Delta'$), if there exists $g \in \mathcal{G}$ such that $\Delta = g\Delta'$.

A **catalogue** is any finite set $\{\Delta(0), \Delta(1), \ldots, \Delta(N-1)\}$ of inequivalent dressed domains. Note that a catalogue need not contain a complete set of representatives from each class, i.e., N may be strictly less than the number of classes. In order to test equivalence, we shall adopt a specific **canonical form.** For $p/q = 1/14$, if $\Delta(n) = (\mathcal{D}(n), \rho(n))$, we require that $\mathcal{D}(n)$ takes the form (cf. (4))

$$\mathcal{D}((7, m_1, m_2), (1, 1, 1), (0, 0, 1))$$

with

$$(m_1, m_2) \in \{(1, 9), (1, 10), (1, 11), (1, 12), (2, 11)\}.$$

It can be shown that this canonical form is well-defined, that is, that in each class there is precisely one domain in canonical form.

The above equivalence generalizes the concept of similarity which proved so useful in the quadratic models [29]. There, a *scaling domain* was defined (in the language of the present article) as a dressed domain with a dressed sub-domain similar to it (i.e., equivalent with respect to the scaling transformation S_ω). Once one understands the dynamics and invariant geometric structures of the scaling domain, one can infer the corresponding properties of the similar sub-domain, and from there, by induction, the properties of an infinite nested set of sub-domains converging to a limit point. In the $p/q = 1/14$ model, the analogous concept of scaling domain is a dressed domain which is the root of an infinite tree of dressed domains with a finite-order recursion algorithm. In other words, the entire infinite tree can be generated from a finite part of it. The following definition makes the idea precise, building in as well the notion of recursive tiling sketched in the introduction.

Definition 1 *A catalogue $\{\Delta(0), \ldots, \Delta(N-1)\}$ is said to satisfy the* **recursive tiling property** *if for each $\Delta(n) = (\mathcal{D}(n), \rho(n))$ there exist dressed sub-domains $\Delta(n, k)$, $k = 0, \ldots, K(n)-1$ and cells $\Pi(n, m)$, $m = 0, \ldots, M(n)$, such that each $\Delta(n, k)$ is equivalent to some member of the catalogue, and moreover $\mathcal{D}(n)$ is partitioned by the return orbits of the $\Delta(n, k)$ and $\Pi(n, m)$ with respect to $\rho(n)$.*

Key parameters in a catalogue are the **scaling factors** $\omega = \omega(n, k)$ corresponding to the group element $g \in \mathcal{G}$ that transforms $\Delta(n, k)$ into the equivalent catalogue member —cf. equations (6,7) and (9) below. Of relevance are also the discontinuity set and residual set in each catalogue member, denoted by $\Gamma(n)$ and $\Sigma(n)$, respectively.

In Figure 2 we show an instance of a partition of a catalogue into return orbits $\mathcal{U}$ and periodic orbits $\mathcal{P}$. For the former we use the notation

$$\mathcal{U}(n, k) = \bigcup_j \mathcal{U}_j(n, k) \tag{8}$$

and assign to each of these sets a specific colour. The white polygons correspond to the periodic orbits $\mathcal{P}_j$. Examples of the equivalence relations involved in the definition of recursive tiling are given in Figure 3.

With the above terminology, the scaling domains of any one of the quadratic models in [29] are equivalent to members of a catalogue of dressed domains with the recursive tiling property. In each case, every prototype $\Delta(n)$ has a single dressed sub-domain $\Delta(n,0)$ equivalent to it. Moreover, there exist minimal catalogues, each containing a single element $\Delta(0)$ similar to its sub-domain $\Delta(0,0)$. In [29], the property of recursive tiling was not spelled out explicitly, but rather was the consequence of computer-assisted proofs.

We summarize some important consequences of the recursive tiling property in the following

Proposition 1 *Let* $\{\Delta(0), \ldots, \Delta(N-1)\}$ *be a catalogue of dressed domains with the recursive tiling property. Then*

- *(i) Each* $\Delta(n)$ *is the root of an infinite tree of dressed sub-domains* $\Delta(n, k_1, \ldots, k_L)$*.*
- *(ii) For fixed* n *and* k*, let* $\mathcal{U}(n,k)$ *be the union of the domains in the return orbit of* $\Delta(n,k)$*. The* $\mathcal{U}(n,k)$ *are mutually disjoint subsets of* $\mathcal{D}(n)$ *which cover* $\Sigma(n)$*. These subsets can be further partitioned, by the recursive tiling, into mutually disjoint subsets* $\mathcal{U}(n, k_1, \ldots, k_L)$*, defined as the union of the domains in the return orbit of* $\Delta(n, k_1, \ldots k_L)$ *with respect to* $\rho(n)$*. For fixed "level"* L*, the* $\mathcal{U}(n, k_1, \ldots, k_L)$ *together cover* $\Sigma(n)$*.*
- *(iii) For any* L*, the sets* $\mathcal{U}(n, k_1, \ldots, k_L) \cap \Sigma(n)$ *are mutually disjoint,* $\rho(n)$*-invariant, and together exhaust* $\Sigma(n)$*.*

The covering $\mathcal{U}(n, k_1, \ldots, k_L)$ of the residual set is partitioned into the domains $\mathcal{D}_j(n, k_1, \ldots, k_L)$ and their return orbits. We shall refer to them as **tiles.**

Proof of Proposition 1. The infinite tree property follows by induction. The disjointness of the sets $\mathcal{U}(n,k)$, or, more generally, of the $\mathcal{U}(n, k_1, \ldots, k_L)$ for fixed L, follows from item *(ii)* of Definition 1. The disjointness and completeness in *(iii)* follow directly from those properties of $\mathcal{U}(n, k_1, \ldots, k_L)$.

To obtain the $\rho(n)$-invariance, let $\zeta \in \mathcal{U}(n, k_1, \ldots, k_L)$; then clearly $\rho(n)\zeta$ lies in $\mathcal{U}(n, k_1, \ldots, k_L)$ unless it is on a boundary point of one of the tiles. By throwing out all the preimages of these boundary points, we make the resulting set, $\mathcal{U}(n, k_1, \ldots, k_L) \setminus \Gamma$, invariant. Since $\overline{\Gamma}$ is also invariant, we get the result. $\square$

It follows from the construction that to every point of Σ there corresponds a unique nested sequence of tiles. Each step along this sequence corresponds geometrically to restricting oneself to a tile of the next level, specified symbolically by an additional triple of indices (k, j, t). Recently, Poggiaspalla [36] studied such sequences and their symbolic dynamics in the important case of self-similar symbol sequences, identifying the dynamics as a Vershik map on a stationary Bratteli diagram and deriving results concerning their ergodic and fractal properties. The formalism of [36] applies to all of the quadratic models studied thus far, and to a restricted subset of Σ in the cubic $\pi/7$ model.

For the unrestricted $\pi/7$ model, the appropriate symbolic dynamics has been worked out, and it has been possible [30] to prove unique ergodicity for the infinitely many minimal invariant components of Σ.

3 Recursive tiling of the $\pi/7$ model

In this section we state and prove our main tiling result, for two different maps with cubic parameters. The first example has as its starting point a triangular dressed domain with a tri-partite domain map. Such a case has been the object of intensive numerical and analytical investigation [22]. The second example, with an initial square domain, was motivated by analogous maps studied in the quadratic cases [29] and by the investigation of π/n models by Kahng [27]. In each example, the choice of dressed domains needed to complete the catalogue was far from obvious, and required a lengthy computer-assisted search. One feature which made the search particularly treacherous was the need to weed out domains with infinite return-map partitions. Furthermore, the catalogue itself is highly non-unique, and presumably arbitrarily large catalogue can be constructed; the identification of relevant invariants and canonical forms is therefore an important open problem. To extend our formalism to a broad class of models will clearly require the development of more powerful, highly automated software to help in the discovery and the exploration of recursive tiling catalogues.

In what follows, a catalogue $\{\Delta(n)\}$ will be defined with data tables specifying its prototypes $\Delta(n)$, tiles $\mathcal{D}_i(n)$, dressed sub-domains $\Delta(n,k)$, and cells $\Pi_j(n)$. For reasons of space, part of these data are available only in the electronic supplement [34].

3.1 Tiling a triangle

We consider first the triangular domain (cf. Equation (4))

$$\Omega = \mathcal{D}((7,2,11),(1,1,1),(0,0,1)),$$

with domain map ρ given by $T_{\delta_i}^{\nu_i} \circ C$ on the sub-domain Ω_i, $i = 0,1,2$, where

$$\begin{array}{lll} \Omega_0 = \mathcal{D}((3,11,7),(1,1,1),(-\tau,1,0)) & \nu_0 = 10 & \delta_0 = (-\tau,-1), \\ \Omega_1 = \mathcal{D}((11,2,7),(1,1,1),(\tau,0,0)) & \nu_1 = 0 & \delta_1 = (1-\tau,-3+\lambda^2), \\ \Omega_2 = \mathcal{D}((4,2,10),(1,1,1),(-\tau,0,\tau)) & \nu_2 = 2 & \delta_2 = (1-\tau,\tau), \end{array}$$

with $\tau = \lambda^{-1} = 2+\lambda-\lambda^2$. The following theorem shows that the dressed domain $\Delta(0) = (\Omega,\rho)$ is a member of a catalogue with the recursive tiling property.

Theorem 2 *The catalogue $\{\Delta(0),\Delta(1),\Delta(2)\}$ defined in Tables 1–4 has the recursive tiling property, with units as scaling factors.*

The prototype domains, with their respective partitions, dressed sub-domains, and tilings are illustrated in Figures 1 and 2. The sub-domain equivalence relations listed in Table 1 are displayed as a graph in Figure 3(a).

The computer-assisted proof is documented in Part 3 of the electronic supplement to this article [34]. The proof consists of first validating the information in the tables, and then verifying that each of the criteria in the definition of scaling domain is satisfied. We rely on a Mathematica-based computer assistant developed in [29], equipped with functions `rotate`, `reflect`, `translate`, and `rescale` to effect the named operations on domains, functions `subdomain`, `equal`, and `disjoint` to check relations between domains, and a function `area` to calculate the area of a domain. All functions are evaluated exactly, using only arbitrary precision integer arithmetic and symbolic computation to manipulate polynomial expressions in λ. The latter are simplified at every stage in the computation by applying (1) and (2).

3.2 Tiling a square

Here we consider an alternative starting point, namely the domain $\Omega = [0,\tau)^2$ with domain map $T_{\delta_i} \circ C$ on the component Ω_i, where

$$\begin{array}{ll} \Omega_0 = \mathcal{D}((0,1,2),(-1,1,-1),(0,\tau,\tau)) & \delta_0 = (0,-\tau) \\ \Omega_1 = \mathcal{D}((0,2,1,0,2),(-1,1,1,1,-1),(0,\tau,\tau,\tau,0)) & \delta_1 = (0,0) \\ \Omega_2 = \mathcal{D}((0,2,1),(1,1,-1),(\tau,0,0)) & \delta_2 = (0,\tau) \end{array}$$

where $\tau = \lambda^{-1} = 2 + \lambda - \lambda^2$. The domain-map partition is shown in Figure 4.

To obtain a recursive tiling of Ω, it is sufficient to show that the domain Ω_2, equipped with its first-return map, is a member of a catalogue with the recursive tiling property. That is because the forward images of the tiles of Ω_2 cover all of Ω, except for a set of dimension 1 (see Figure 5). We note that Ω_2, with its domain map, is equivalent to the prototype dressed domain $\Delta(0)$ in Table 5.

Theorem 3 *The catalogue $\{\Delta(0),\ldots,\Delta(3)\}$ defined in Table 5 and Part 4 of [34] has the recursive tiling property, with units as scaling factors.*

The catalogue of prototype domains needed to construct the complete scaling tree of cells includes, in addition to $\Delta(0)$ itself and the same $\Delta(1)$ and $\Delta(2)$ encountered in the triangular case, an additional dressed domain $\Delta(3)$. The dynamical partitions of the new prototypes are shown in Figure 6, while in Figure 3(b) we display the graph of sub-domain relations for the catalogue. A complete set of data tables for the catalogue, together with additional figures showing the sub-domain and tiling relations, and a computer-assisted proof of the theorem, are contained in parts 4 and 5 of the electronic supplement to this article [34].

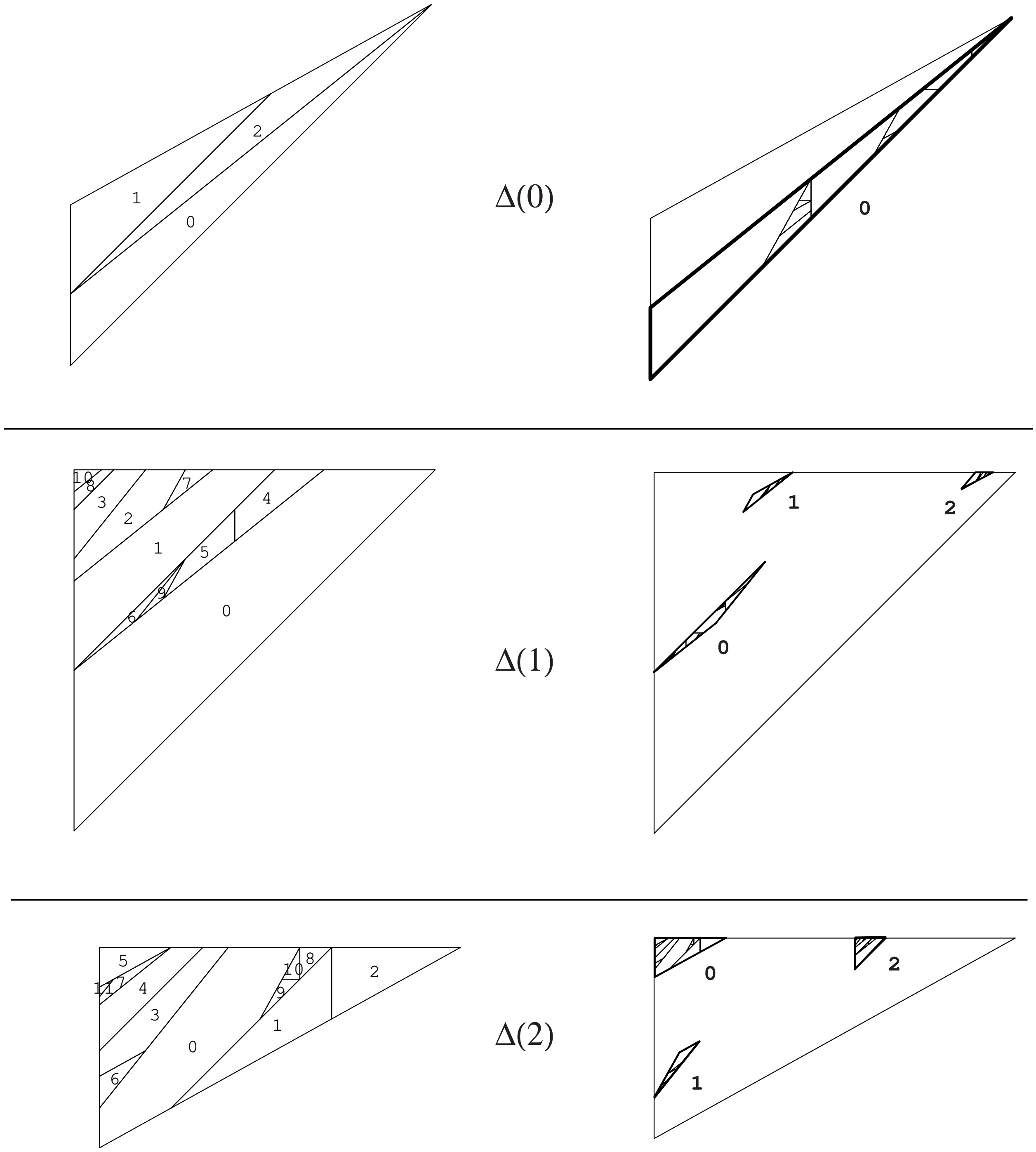

Figure 1: The catalogue of Theorem 2. Each of the three prototypes $\Delta(n)$ is shown with its tiles $\mathcal{D}_j(n)$, labelled by the integer j (left), and its dressed sub-domains $\Delta(n,k)$, labelled by k (right).

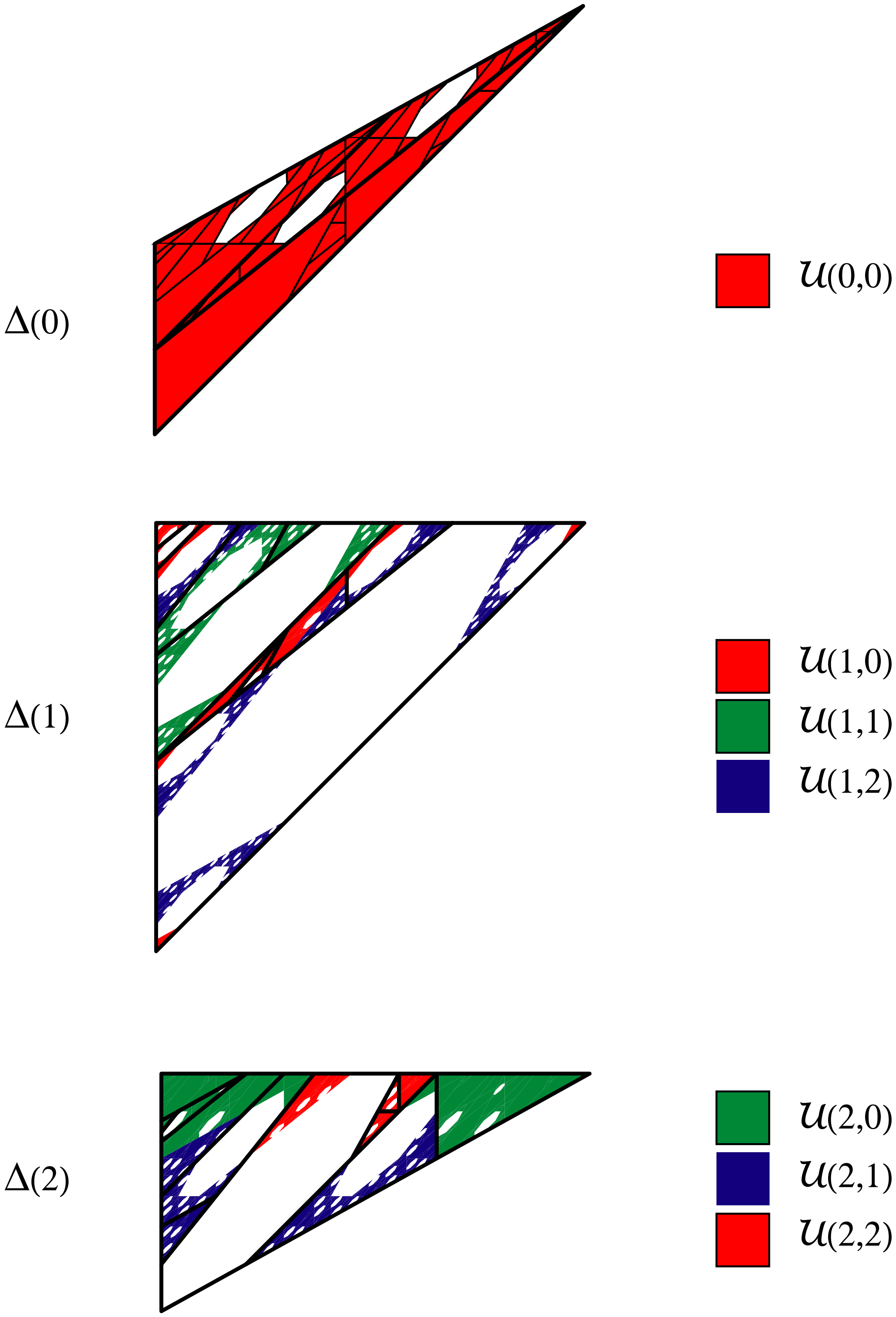

Figure 2: Partition of the catalogue of Theorem 2. Each prototype domain $\Delta(n)$ is tiled by sub-domain tiles $\mathcal{D}_j(n,k)$ and periodic cells $\Pi_j(n)$. The colour-coded quantity $\mathcal{U}(n,k)$, defined in Equation (8), is the return orbit of $\Delta(n,k)$ in $\Delta(n)$.

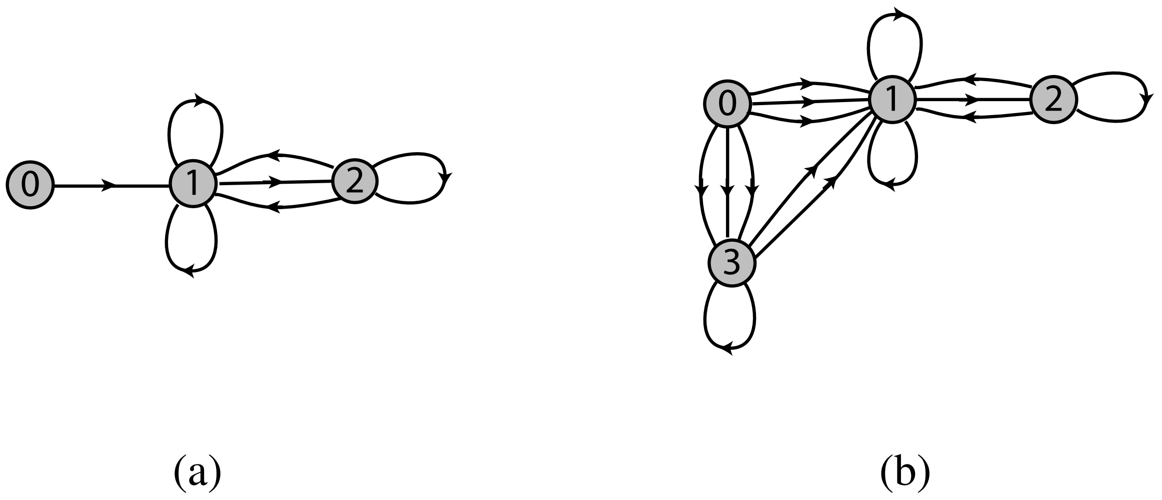

Figure 3: Graphs representing the sub-domain relations, for the recursive tiling of the (a) triangle (Table 1), and (b) square (Table 5). The vertex n represents the domain prototype $\Delta(n)$ in the corresponding catalogue. An oriented arc connecting two vertices indicates that a sub-domain of the first vertex is equivalent to the second vertex, under the action of the group $\mathcal{G}$ defined in Equation (7).

4 Fractal geometry

In this section we derive some fractal properties of a catalogue of dressed domains satisfying the recursive tiling property. We first prove a general theorem giving a sufficient condition for the equality of Hausdorff and box-counting dimensions and the existence of a finite, non-zero Hausdorff measure for each of the domains of the catalogue and each of their respective tiles. The statement of the theorem includes an equation for the dimension in terms of the recursive tiling data. For the examples studied in the previous section, it is straightforward —with computer assistance— to verify the hypothesis of the theorem and to write down a transcendental equation for the dimension. Finally, we show that the nontrivial Hausdorff measure for the tiles easily extends to infinitely many disjoint invariant subsets of the residual set, thus establishing the existence of infinitely many invariant components.

4.1 Notation

We introduce some notation concerning catalogues with the recursive tiling property. (cf. Definition 1 and Proposition 1). First of all, each dressed sub-domain is equivalent, under the group $g \in \mathcal{G}$ (equation 7), to a unique catalogue member . This equivalence defines implicitly a function $h = h(n,k)$

$$\Delta(n,k) \sim \Delta(h(n,k)). \tag{9}$$

Under the domain map $\rho(n,k)$, the domain $\mathcal{D}(n,k)$ is partitioned into sub-domains (level-1 tiles) $\mathcal{D}_j(n,k), j = 0,\ldots,J(n,k)$, where $J(n,k) = J(h(n,k))$. Applying the recursion L times produces dressed sub-domains $\Delta(n,k_1,\ldots,k_L)$, with corresponding level-L tiles, $\mathcal{D}_j(n,k_1,\ldots,k_L), j =$

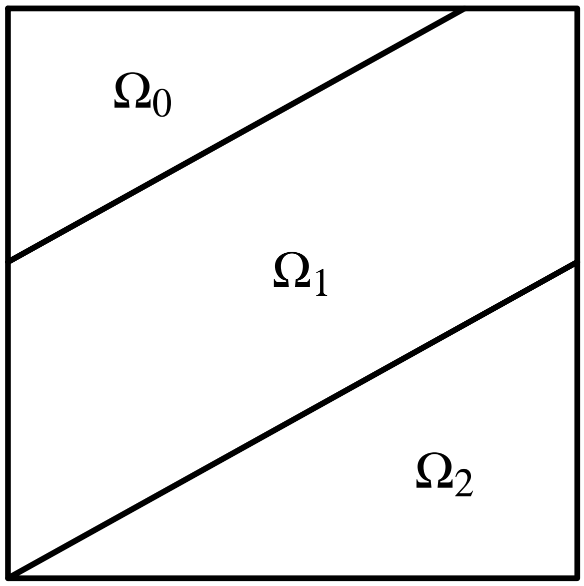

Figure 4: Domain-map partition of the square.

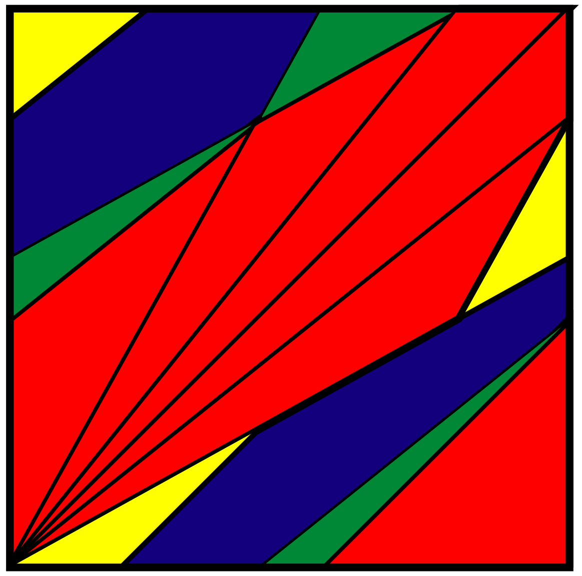

Figure 5: Tiling of the square by sub-domains of Ω_2.

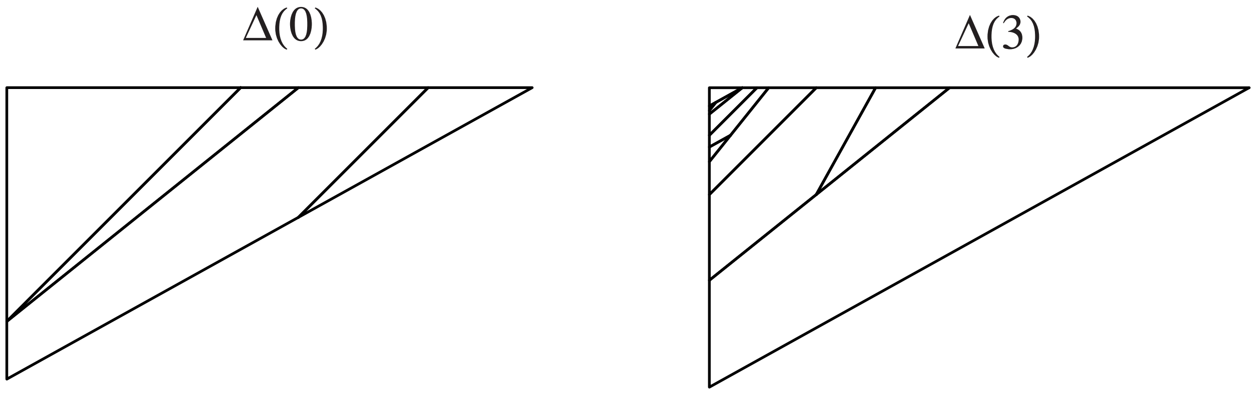

Figure 6: The catalogue of Theorem 3, showing the two prototypes $\Delta(0)$ and $\Delta(3)$ and their tiles, defined in Table 5. In addition, the catalogue includes the prototypes $\Delta(1)$ and $\Delta(2)$ displayed in Figure 1.

$0, \ldots, J(n, k_1, \ldots, k_L)$. The function $h(n, k_1, \ldots, k_L)$ is defined recursively by the equivalence

$$\Delta(n, k_1, \ldots, k_L) \sim \Delta(h(n, k_1, \ldots, k_L)).$$

Clearly

$$h(n, k_1, \ldots, k_L) = h(h(n, k_1, \ldots, k_{L-1}), k_L),$$

and

$$J(n, k_1, \ldots, k_L) = J(h(n, k_1, \ldots, k_L)).$$

The fundamental scaling factors characterizing the recursive tiling are the ratios

$$\omega(n, k) = |\, \mathcal{C}^{\nu}\mathcal{D}(n, k)\, | \,/\, |\, \mathcal{D}(h(n, k))\, |$$

where $|\mathcal{D}| = \sup\{|x - y| : x, y \in \mathcal{D}\}$ is the diameter of $\mathcal{D}$, and $\mathcal{C}^{\nu}$ is the generalized rotation which brings $\mathcal{D}(n, k)$ into similarity with $\mathcal{D}(h(n, k))$ (cf. remark following Definition 1). For a true rotation, the diameter is orientation-independent, and so the rotation can be omitted. Scale factors for higher-level tiles can be introduced recursively

$$\omega(n, k_1, \ldots, k_L) = \omega(n, k_1, \ldots, k_{L-1})\, \omega(h(n, k_1, \ldots, k_{L-1}),\, k_L)$$

from which one sees that if the catalogue scaling factors are units, so are all higher-level scaling factors.

For the purpose of counting tiles, we denote by $A_{i,j}(n, k)$ the number of tiles of the form $\rho(n)^t \mathcal{D}_j(n, k)$ with $0 \le t < t_j(n, k)$ that are contained in $\mathcal{D}_i(n)$. Further, we define $A_{i,j}(n, k_1, \ldots, k_L)$ to be the number of distinct images (under iteration of the domain map $\rho(n)$) of the tile $\mathcal{D}_j(n, k_1, \ldots, k_L)$ contained in $\mathcal{D}_i(n)$. This can be expressed recursively in terms of the fundamental tile-counting matrix $A_{i,j}(n, k)$

$$A_{i,j}(n, k_1, \ldots, k_L) = \sum_{j_1} A_{i,j_1}(n, k_1, \ldots, k_{L-1}) A_{j_1,j}(h(n, k_1, \ldots, k_{L-1}),\, k_L).$$

A related matrix is the *transfer matrix* $\mathbf{M}(s)$, $s > 0$, whose coefficients are

$$M_{(n_1,j_1),(n_2,j_2)}(s) = \sum_{k} A_{j_1,j_2}(n_1, k)\, \delta_{n_2, h(n_1,k)}\, \omega(n_1, k)^s \tag{10}$$

where δ is Kronecker's delta. Here we consider the pair (n, j) as a single matrix index.

Finally, the s-dimensional Hausdorff measure of a set $\mathcal{D}$ is defined as

$$\mathcal{H}^s(\mathcal{D}) = \lim_{\delta\to 0} \mathcal{H}^s_\delta(\mathcal{D}) \qquad \mathcal{H}^s_\delta(\mathcal{D}) = \inf\left\{\sum_{i=1}^{\infty} |U_i|^s \,:\, \{U_i\} \text{ is a } \delta\text{-cover of } \mathcal{D}\right\}$$

while its Hausdorff dimension is defined in terms of the measure as $\dim_H \mathcal{D} = \inf\{s : \mathcal{H}^s(\mathcal{D}) = 0\}$ (see, e.g., [14, Chapter 2]). Lower and upper box-counting dimensions are defined by [14, Chapter 3]

$$\underline{\dim}_B\mathcal{D} = \underline{\lim}_{\delta\to 0}\frac{\log N_\delta(\mathcal{D})}{-\log\delta}, \quad \overline{\dim}_B\mathcal{D} = \overline{\lim}_{\delta\to 0}\frac{\log N_\delta(\mathcal{D})}{-\log\delta},$$

where $N_\delta(\mathcal{D})$ is the smallest number of sets of diameter at most δ which can cover $\mathcal{D}$. These satisfy [14]

$$\dim_H \mathcal{D} \le \underline{\dim}_B\mathcal{D} \le \overline{\dim}_B\mathcal{D}.$$

If $\underline{\dim}_B\mathcal{D} = \overline{\dim}_B\mathcal{D}$, $\dim_B \mathcal{D}$ is defined as their common value.

4.2 Theorem on dimensions and measures

Theorem 4 *Let $\mathbf{M}(s)$ be the transfer matrix for a catalogue with recursive tiling. Suppose that, for some $s = s_0$, $1 < s_0 \le 2$, there exists an $\mathbf{M}(s_0)$-invariant vector ψ whose components are all strictly positive and sum to unity. Then, for any tile $\mathcal{D}$ of any catalogue member $\Delta(n)$, the Hausdorff and box-counting dimensions of $\overline{\Gamma}(n) \cap \mathcal{D}$ (and of $\Sigma(n) \cap \mathcal{D}$) are equal to s_0, and the corresponding Hausdorff measures are finite and non-zero. The dimension s_0 is a solution of the equation* $\det(\mathbf{1} - \mathbf{M}(s)) = 0$.

Proof. The underlying generalized rotation matrix C is assumed to be linearly conjugate to a rotation by $2\pi p/q$, $p, q \in \mathbf{Z}$. Without loss of generality, we can assume that the matrix C is a true rotation. This is because the matrix elements of $\mathbf{M}(s)$ are unaffected by the linear conjugacy, and the dimension and non-triviality of measure are also unchanged, since the conjugacy is a bi-Lipschitz transformation.

Under the hypothesis of the theorem, the equation for s_0 follows from linear algebra. To establish the remaining results, we shall adapt the proof of Theorem 9.3 of [14], which establishes analogous properties of fractals constructed from similarity transformations. We shall first obtain an upper bound for the s_0-dimensional Hausdorff measure, then get the more elusive lower bound to complete the proof that s_0 is the Hausdorff dimension with finite, non-zero Hausdorff measure. Then we will show that the upper box-counting dimension (which must be at least s_0) is in fact also bounded above by s_0, hence equal to it.

The key ingredient to the proof is the introduction of a mass distribution (finite measure) μ on each catalogue member $\Delta(n) = (\mathcal{D}(n), \rho(n))$. We start with the set $\mathcal{S}$ consisting of arbitrary-level tiles and cells, their edges and vertices, as well as $\mathcal{D}(n)$ and the empty set. This set is a semi-ring, in that it is closed under intersection, and for all $A, B \in \mathcal{S}$ such that $B \subset A$, the set $A \setminus B$ is a finite or countable union of disjoint elements of $\mathcal{S}$.

These properties are immediate consequences of the recursive tiling structure. We define a function μ on $\mathcal{S}$, by letting, for all indices $n, j, t, L, k_1, \ldots, k_L$ in their respective ranges

$$\begin{array}{ll} \text{(a)} & \mu(A) = 0 \text{ if } A \text{ is a cell, edge, vertex or the empty set} \\ \text{(b)} & \mu(\rho(n)^t \mathcal{D}_j(n)) = \psi_{(n,j)} > 0, \\ \text{(c)} & \mu(\mathcal{D}(n)) = \sum_{j=0}^{J(n)-1} \psi_{(n,j)} = 1, \\ \text{(d)} & \mu(\rho(n)^t D_j(n, k_1, \ldots, k_L)) = \omega(n, k_1, \ldots, k_L)^{s_0} \mu(\mathcal{D}_j(h(n, k_1, \ldots, k_L))). \end{array} \tag{11}$$

The function μ is a probability measure, since $\mu(\emptyset) = 0$, μ is monotone and σ-additive on $\mathcal{S}$, and μ is normalized by assumption. The σ-additivity need only be verified for recursive-tiling partition, since every partition of an element of $\mathcal{S}$ into a finite or countable number of subsets in $\mathcal{S}$ can be constructed via a sequence of recursive tiling partitions. The additivity of the latter is expressed by the identity

$$\sum_{k_L, j} A_{i,j}(h(n, k_1, \ldots, k_{L-1}),\, k_L) \mu(\mathcal{D}_j(n, k_1, \ldots, k_L)) = \mu(\mathcal{D}_i(n, k_1, \ldots, k_{L-1}))$$

which is an instance of

$$\sum_{k,j} A_{i,j}(n,k) \omega(n,k)^{s_0} \mu(\mathcal{D}_j(h(n,k)) = \mu(\mathcal{D}_i(n)). \tag{12}$$

From defining relation (d), for $L = 1$, the left-hand side becomes

$$\sum_{n',j} M_{(n,i),(n',j)} \mu(\mathcal{D}_j(n')) = (\mathbf{M} \cdot \psi)_{(n,i)} = \psi_{(n,i)},$$

from the hypothesis of the theorem. Defining relation (b) then gives us the desired result.

In standard fashion, the measure μ can be extended to a σ-ring $\mathcal{R}$ of subsets of $\mathcal{D}(n)$ which includes finite and countable unions of elements of $\mathcal{S}$ as well as closed balls (restricted to $\mathcal{D}(n)$). If B is one of the latter, one can easily construct a sequence of coverings $\mathcal{C}$ of B by finite numbers of elements of $\mathcal{S}$, for example by means of successively higher-level partitions of $\mathcal{D}(n)$ by cells, tiles and their respective edges and vertices, with all sets disjoint from B omitted. Then $\mu(B)$ is the outer measure,

$$\mu(B) = \inf_{\mathcal{C}} \left\{ \sum_i \mu(A_i) : A_i \in \mathcal{C} \right\}.$$

Note that B is not necessarily the limit of $\bigcup_{A \in \mathcal{C}} A$, since B might intersect a cell Π, and Π will not be further partitioned as one goes to higher levels. Since $\mu(\Pi) = 0$, this does not prevent the outer measure from being well defined.

We note that μ is supported on $\overline{\Gamma}$, a simple consequence of defining relation (a) and the σ-additivity of μ:

$$\begin{array}{rcl} \mu(\mathcal{D}(n)) & = & \mu\left(\bigcup_{\text{cells}} \Pi \cup (\overline{\Gamma}(n) \cap \Gamma(n)) \cap \Sigma(n)\right) \\ & = & \sum_{\text{cells}} \mu(\Pi) + \mu\left(\overline{\Gamma}(n) \cap \Gamma(n)\right) + \mu(\Sigma(n)) \\ & = & \mu(\Sigma(n)). \end{array}$$

Here we have used that the discontinuity set is a countable union of edges and vertices, each of vanishing μ measure, so that

$$\mu\left(\overline{\Gamma}(n) \cap \Gamma(n)\right) \leq \mu(\Gamma(n)) = \sum_{A \in \Gamma(n)} \mu(A) = 0.$$

Clearly the support property holds for each tile $\mathcal{D}$ as well:

$$\mu(\mathcal{D}) = \mu(\mathcal{D} \cap \Sigma(n)).$$

We now proceed to obtain an upper bound for $\mathcal{H}^{s_0}(F)$, where F is either of the sets $\overline{\Gamma}(n) \cap \mathcal{D}_i(n)$ or $\Sigma(n) \cap \mathcal{D}_i(n)$. Thanks to the identities

$$|\overline{\mathcal{D}}| = |\mathcal{D}|, \qquad \mu(\overline{\mathcal{D}}) = \mu(\mathcal{D})$$

where $\overline{\mathcal{D}}$ is the closure of $\mathcal{D}$, the same arguments hold for the two choices of F. For any $\delta > 0$, there exists an $L > 0$ such that the closure of the union of the orbits of all $\mathcal{D}_j(n, k_1, \ldots, k_L)$ is a δ-cover for F. Thus $\mathcal{H}^{s_0}_\delta(F)$ is bounded above by

$$\sum_{k_1,\ldots,k_L} A_{i,j}(n, k_1, \ldots, k_L) \; |\mathcal{D}_j(n, k_1, \ldots, k_L)|^{s_0}.$$

But the diameter scales as

$$|\mathcal{D}_j(n, k_1, \ldots, k_L)| = \omega(n, k_1, \ldots, k_L) \, |\mathcal{D}_j(h(n, k_1, \ldots, k_L))|$$

and all of the $|\mathcal{D}_j(n)|$ satisfy bounds

$$|\mathcal{D}_j(n)| \leq \kappa \mu(\mathcal{D}_j(n))$$

with $\kappa > 0$ independent of n and j. Hence

$$\mathcal{H}^{s_0}_\delta(F) \leq \kappa \sum_{k_1,\ldots,k_L} A_{i,j}(n, k_1, \ldots, k_L) \omega(n, k_1, \ldots, k_L)^{s_0} \mu(\mathcal{D}_j(h(n, k_1, \ldots, k_L))).$$

Introducing the recursion relations for the $A_{i,j}(n, k_1, \ldots, k_L)$ and $\omega(n, k_1, \ldots, k_L)$ and the definition of the transfer matrix (10), the right-hand side of the above inequality can be transformed into

$$\kappa(\mathbf{M}^L \cdot \psi)_{(n,j)} = \kappa \psi_{(n,j)}.$$

and thus we have the δ-independent bound

$$\mathcal{H}^{s_0}_\delta(F) \leq \kappa \Psi, \qquad \Psi = \max\{\psi_{(n,j)} \;:\; n = 0, \ldots, N-1, \;\; j = 0, \ldots, J(n)\},$$

and so

$$\mathcal{H}^{s_0}(F) \leq \kappa \Psi.$$

We now turn to the problem of a lower bound. Let B be a ball of radius r, and construct a set Q by means of the following algorithm. Start with $Q = \{\mathcal{D}_j(n)\}$. Update Q by examining each element D, an image of the tile $\mathcal{D}_j(n, k_1, \ldots, k_L)$ for some L. If $\omega(n, k_1, \ldots, k_L)$ is less than r, keep D; otherwise replace it with all of its level-$(L+1)$ sub-tiles. Repeat the updating until all of the elements have $\omega(n, k_1, \ldots, k_L)$ less than r. This requires a finite number of steps and leaves all elements of the final Q with scales in the interval $(\epsilon r, r]$, where $\epsilon = \min\{\omega(n, k)\}$. Note that placing uniform upper and lower bounds on $\omega(n, k_1, \ldots, k_L)$ simultaneously places uniform bounds on the diameters $|\mathcal{D}_j(n, k_1, \ldots, k_L)| = \omega(n, k_1, \ldots, k_L)|\mathcal{D}_j(h(n, k_1, \ldots, k_L))|$ and the masses $\mu(\mathcal{D}_j(n, k_1, \ldots, k_L)) = \omega(n, k_1, \ldots, k_L)^{s_0}\mu(\mathcal{D}_j(h(n, k_1, \ldots, k_L)))$.

Next, we define Q_1 to be the subset of Q consisting of all elements which intersect the ball B. According to [14, Lemma 9.2], Q_1 contains at most q elements, where q is independent of r. This gives us an upper bound on the mass contained in the ball:

$$\mu(B) \leq \mu\left(\bigcup_{\mathcal{D}\in Q_1} \mathcal{D}\right) \leq \sum_{\mathcal{D}\in Q_1} \mu(\mathcal{D}) \leq c r^{s_0}$$

where $c = q \max\{\mu(\mathcal{D}_j(n))\} = q\Psi$. Since any set U is contained in a ball of radius $|U|$, we have

$$\mu(U) \leq c|U|^s.$$

By the mass distribution principle [14, Section 4.1], this implies

$$\mathcal{H}^{s_0}(F) \geq \mu(\mathcal{D}_i(n))/c.$$

From this estimate and the upper bound achieved above, we conclude that for each level-zero tile, s_0 is the Hausdorff dimension and that the Hausdorff measure of dimension s_0 is non-zero and finite. The result is extended to tiles of arbitrary level by scaling:

$$\mathcal{H}^{s_0}(\overline{\Gamma}(n) \cap \mathcal{D}_j(n, k_1, \ldots, k_L)) = \omega(n, k_1, \ldots, k_L)^{s_0}\mathcal{H}^{s_0}(\overline{\Gamma}(n) \cap \mathcal{D}_j(h(n, k_1, \ldots, k_L))),$$

and the analogous identity with $\overline{\Gamma}(n)$ replaced by $\Sigma(n)$.

In the final segment of the proof, we show that the Hausdorff and box-counting dimensions are equal. For all $\mathcal{D}$, isometric to $\mathcal{D}_j(n, k_1, \ldots, k_L) \in Q$, we have

$$|\mathcal{D}| = |\mathcal{D}_j(n, k_1, \ldots, k_L)| \leq \gamma r,$$

where $\gamma = \max|\mathcal{D}_j(n)|$. On the other hand, the lower bound for $\mu(\mathcal{D})$, $\mathcal{D} \in Q$, when summed over all N_Q elements, gives

$$N_Q(\epsilon r)^{s_0} \leq \xi \sum_{\mathcal{D}\in Q} \mu(\mathcal{D}) = \xi\mu(\mathcal{D}_j(n)) \leq \xi,$$

where $\xi = (\min \mu(\mathcal{D}_j(n)))^{-1}$ and we have used the additivity of the measure (recall no mass was lost in the construction of Q) as well as its normalization. Thus F can be covered by $\lfloor \xi(\epsilon r)^{-s} \rfloor$ sets of diameter γr. Since r can be made arbitrarily small, this establishes

$$\overline{\dim}_B F \leq s_0,$$

and hence the equality of box-counting and Hausdorff dimensions. $\square$

In the proof of Theorem 4, we introduced a measure μ defined on a σ-ring $\mathcal{R}$ of subsets of $\mathcal{D}(n)$, with support on $\overline{\Gamma}(n)$. This measure induces an invariant measure $\hat{\mu}$ on $\Sigma(n)$ whose properties are stated in the following

Corollary 5 *Under the hypotheses of Theorem 4, the measure μ defined by (11) induces a measure $\hat{\mu}$ on $\Sigma(n)$ with associated σ-ring $\hat{\mathcal{R}}$ generated by sets of the form $\Sigma \cap \mathcal{D}$, $\mathcal{D}$ a tile. This measure is invariant with respect to the domain map $\rho(n)$. If $\rho(n) = T_\delta \circ C^\nu$, C a true rotation, then, for all $A \in \hat{\mathcal{R}}$,*

$$\hat{\mu}(A) = \frac{\mathcal{H}^{s_0}(A)}{\mathcal{H}^{s_0}(\Sigma(n))}.$$

Proof. It is straightforward to show that the identity

$$\hat{\mu}(\Sigma(n) \cap \mathcal{D}) \stackrel{\text{def}}{=} \mu(\mathcal{D})$$

defines a measure on $\Sigma(n)$ with the stated σ-ring. The edges and vertices in the original semi-ring for μ are, of course, absent since they do not intersect $\Sigma(n)$.

To prove the invariance of $\hat{\mu}$, it is sufficient to show $\hat{\mu}(\rho(n)^{-1}\hat{\mathcal{D}}) = \hat{\mu}(\hat{\mathcal{D}})$, where $\hat{\mathcal{D}}$ is the restriction to $\Sigma(n)$ of a tile $\mathcal{D}$. It is useful here to distinguish tiles $\rho(n)^t\mathcal{D}_j(n, k_1, \ldots, k_L)$ which are base tiles (t=0) from those which are not ($0 < t < T_j(n, k_1, \ldots, k_L)$). If $\mathcal{D}$ is a non-base tile or cell, our result is trivial: the inverse image of $\mathcal{D}$ is another tile or cell on the same return orbit, hence has the same μ measure by defining properties (a) and (d). On the other hand, if $\mathcal{D}$ is a base tile, it can be partitioned, via recursive tiling, into a finite set of cells, non-base tiles, and base tiles. It is easy to see that there exists a positive $\epsilon < 1$, independent of $\mathcal{D}$, such that the total μ measure of the base tiles is less than $\epsilon\,\mu(\mathcal{D})$. Repeatedly partitioning the base tiles, one obtains a partition of $\mathcal{D}$ into non-base tiles, cells, and base tiles of arbitrarily small total μ measure. This, together with the already established invariance for non-base tiles and cells, suffices to establish the result for all tiles, hence for the full σ-ring.

We now restrict ourselves to the case of C a true rotation. The system of equations (12) holds if we replace $\mu(\mathcal{D}_j(n))$ by $\hat{\mu}(\hat{\mathcal{D}}_j(n))$ or $\mathcal{H}^{s_0}(\hat{\mathcal{D}}_j(n))$, where $\hat{\mathcal{D}}_j(n) = \mathcal{D}_j(n) \cap \Sigma(n)$. This is based on the additivity of the respective measures and the fact that they are uniform over the return orbit of a basic tile. For $\hat{\mu}$ this follows from defining relation (b) for μ, while for $\mathcal{H}^{s_0}$ it is a consequence of the Euclidean invariance of Hausdorff measure (see [14, Section 2.1]). Thanks to the vanishing of $\det(\mathbf{1} - \mathbf{M}(s_0))$, the system (12) has a unique solution up to overall normalization. Thus, for $A = \hat{\mathcal{D}}_j(n)$, we have

$$\hat{\mu}(A) = \alpha\,\mathcal{H}^{s_0}(A),$$

for some positive constant α, which can be extended to the restriction of any tile by applying the defining relation (d) for μ, and the scaling and Euclidean invariance of Hausdorff measure. The constant of proportionality is determined by the normalization of μ. The same proportionality extends in standard fashion to any $A \in \hat{\mathcal{R}}$.

We note that in the true-rotation case, we could have avoided the cumbersome proof of $\rho(n)$-invariance given above: once the proportionality of measures has been established, the $\rho(n)$-invariance of $\hat{\mu}$ follows from the Euclidean invariance of $\mathcal{H}^{s_0}$. $\square$

4.3 Fractal properties in the $\pi/7$ model

We now apply the results of our theorem to the catalogue $\{\Delta(1), \Delta(2)\}$ with data specified in Tables 1–4 and 6. This is a sub-catalogue of those discussed in the previous section (cf. Figure 3); extending the results to the larger catalogues will present no difficulties.

Our first task is to construct the transfer matrix $\mathbf{M}$ from the $A_{i,j}(n,k)$ listed in Table 6 and the scale factors $\omega(n,k)$, whose inverses are listed in the last column of Table 3. It is helpful to express the $\omega(n,k)$ in terms of the fundamental units (2):

$$\begin{array}{lll} \omega(1,0) = \eta_1^2\eta_2^2 & \omega(1,1) = \eta_1^2\eta_2^2 & \omega(1,2) = \eta_1\eta_2^3 \\ \omega(2,0) = \eta_2^2 & \omega(2,1) = \eta_2^2 & \omega(2,2) = \eta_1^{-1}\eta_2^3. \end{array}$$

The equation for s_0 is then obtained by calculating the determinant of the 23 x 23 matrix $\mathbf{K} = \mathbf{1} - \mathbf{M}(s)$. We get

$$F(\eta_1^s, \eta_2^s) = 0,$$

where the polynomial

$$\begin{aligned} F(x,y) \quad = \quad & 1 - 6\,y^2 - 37\,x^2y^2 - 51\,xy^3 + 9\,y^4 + 92\,x^2y^4 - 29\,x^4y^4 + 71\,xy^5 \\ & -69\,x^3y^5 - 4\,y^6 - 66\,x^2y^6 + 23\,x^4y^6 + 9\,x^6y^6 - 20\,xy^7 - 48\,x^3y^7 \\ & -50\,x^5y^7 + 25\,x^2y^8 + 19\,x^4y^8 - 9\,x^6y^8 + 5\,x^3y^9 - 6\,x^5y^9 - 6\,x^4y^{10} \end{aligned} \tag{13}$$

is irreducible over $\mathbf{Q}$. Using the cubic equation for λ, one can show that

$$\det \mathbf{K}(1) = 20345 + 3096\lambda - 7985\lambda^2 < 0,$$

$$\det \mathbf{K}(2) = -7462700 - 1803627\lambda + 3299289\lambda^2 > 0.$$

Moreover, it is not difficult to place a positive lower bound on the derivative of the determinant in the interval between 1 and 2. Thus, $\det \mathbf{K}(s_0)$ has a simple root between 1 and 2. Using Newton's method with arbitrary precision floating-point arithmetic, one can evaluate the root to any desired accuracy. With 20 significant digits, we have

$$s_0 = 1.6522336518816627081.... \tag{14}$$

To check the hypothesis of the theorem, we must study the vector ψ left invariant by application of $\mathbf{M}$. Using elementary linear algebra, we obtain an exact solution of the system $\mathbf{M}\psi = \psi$, $\sum_{n,j} \psi_{(n,j)} = 1$, with each component expressed as a ratio of polynomials in the quantities $x = \eta_1^{s_0}$ and $y = \eta_2^{s_0}$. To obtain rigorous upper and lower bounds on the components, we use interval arithmetic with rational rounding (for each interval, the upper bound is rounded upward to a rational, and the lower bound is rounded down to a rational). Assigning x and y the bounding intervals

$$\mathcal{I}(x) = (377/1000, 378/1000), \quad \mathcal{I}(y) = (262/1000, 263/1000),$$

we obtain, with computer assistance, the following bounds:

$$\begin{aligned} &[(545,937),(349,377),(311,338),(180,194),(180,194),(167,181), \\ &(73,80),(68,75),(23,27),(43,47),(43,47),(479,525),(1613,1729), \\ &(1651,1778),(927,1003),(1174,1266),(515,556),(332,366), \\ &(247,268),(138,170),(184,199),(150,163),(56,61)] \end{aligned}$$

where the ith integer pair (m_i, n_i) in the above array signifies that the ith component of ψ lies between $m_i/10^4$ and $n_i/10^4$. Thus all components of the $\mathbf{M}$-invariant vector are strictly positive, and so the results of the theorem follow.

Each of the sets $\mathcal{U}(n, k_1, \ldots, k_L) \cap \Sigma(n)$ is invariant with respect to the domain map $\rho(n)$ and, by Theorem 4, has finite, non-zero Hausdorff measure with dimension s_0. Since one can have countably many disjoint sets of this type, and since the contribution of each of them to the total measure can be assigned an independent weight, we conclude that the number of inequivalent invariant measures on $\Sigma(n)$ is infinite.

5 Construction and counting of periodic cells

From Proposition 1, it is clear that one can construct sub-domains $\Delta(n, k_0, k_1, \ldots, k_{L-1})$ and periodic domains (cells) $\Pi(n, k_0, k_1, \ldots, k_{L-1})$ of arbitrary level L. The former are all equivalent to various catalogue domains $\Delta(n)$, while the latter are equivalent to the periodic domains $\Pi_j(n)$. We calculate the level-L return times.

Let $A_{i,j}(n, k_1, \ldots, k_L)$ be the the tile-counting parameters defined in Section 4.1. Further, let $B_{i,j}(n)$ be the number of cells of the form $\rho(n)^t \Pi_j(n)$ that are contained in $\mathcal{D}_i(n)$. We have

Proposition 6 *The return time (in $\Delta(n)$) of the domain $\mathcal{D} = \mathcal{D}(n, k_1, \ldots, k_L)$ is*

$$t_j(n, k_1, k_2, \ldots, k_L) = \begin{cases} \sum_i A_{i,j}(n, k_1, \ldots, k_L) & \mathcal{D} = \mathcal{D}_j \\ \sum_i (A_{i,j}(n, k_1, \ldots, k_L) B_{i,j}(h(n, k_1, \ldots, k_L)) & \mathcal{D} = \Pi_j. \end{cases} \tag{15}$$

We now wish to make an exact count $N(T)$ of the periodic cells with periods (i.e., return times with respect to the level-zero return map $\rho(0)$) less than T, and then explore the asymptotic behaviour of $N(T)$ for large T. The recursive tiling property allows us to organize the periodic orbits into **scaling trees** analogous to the scaling sequences of the quadratic cases. At the root of the tree is a bare cell $\Pi_j(n)$ associated with a particular prototype domain $\Delta(n)$. In the examples of this article, all of the $\Pi_j(n)$ are equivalent to a single heptagon Π, but in other examples this will not be the case; the various $\Pi_j(n)$ could have quite different sizes and shapes. On the other hand, the tree based on $\Pi_j(n)$ consists only of cells equivalent to it, namely those of the form $\Pi_j(n_0, k_0, k_1, \ldots, k_{L-1})$, where the last subscript corresponds to prototype $\Delta(n)$. The periods of these level-L cells are given by $t_j(n_0, k_0, k_1, \ldots, k_{L-1})$ in Proposition 6.

For a numerical calculation of $N(T)$, we add the orbit counts from the various scaling trees. For each of the latter, we build up the matrix products in (15) from right to left, counting the number of orbits whose periods are less than T. Each step in this process involves branching, since in going from (n_r, k_r) to (n_{r-1}, k_{r-1}), there are typically multiple choices for the latter consistent with the relation $n_r = h(n_{r-1}, k_{r-1})$. In the triangular example, the last column of Table 1 tells us that $n_r = 1$ is consistent with (n_{r-1}, k_{r-1}) equal to $(0,0), (1,1), (1,2), (2,0)$, or $(2,2)$, whereas $n_r = 1$ is consistent with (n_{r-1}, k_{r-1}) equal to $(1,0)$ or $(2,1)$.

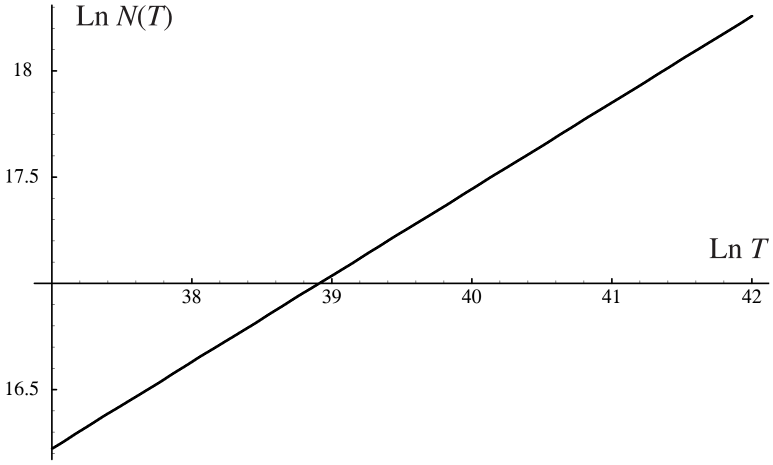

Figure 7: Log-log plot of the number of periodic orbits with period less than T as a function of T.

We have carried out the exact calculation of $N(T)$ for 50000 values of T between e^{37} and e^{42}, approximately equally spaced on a logarithmic scale, with a total of about 7.4×10^7 periodic orbits. The result approximates very well a straight line on a log-log plot (Figure 7), corresponding to the asymptotic power law

$$N(T) \sim 3.204\, T^{0.4070}$$

with an error of at most 0.0001 in the exponent. We plot the fluctuations from the power law in Figure 8.

A similar calculation was be performed to calculate $N'(\epsilon)$, the number of cells of size greater than ϵ, where the latter is the length of the horizontal (or vertical) side of the heptagonal cell (the size of the prototype Π is 1). The structure of the recursive program is the same as for the period-counting, except that now one must keep track at each level of the net scale factor. In going from one level to the next, one must multiply the latter by the appropriate factor ω taken from Table 3.

We made an exact calculation of $N'(\epsilon)$ for 16000 values of ϵ between e^{-36} and e^{-20}, approximately equally spaced on a logarithmic scale. This included approximately 7.5×10^{23} cells located on approximately 1.3×10^6 orbits. A least-squares fit to a straight line on a log-log scale reveals (Figures 9 and 10) a power law

$$N'(\epsilon) \sim 0.0108\, \epsilon^{-1.652}$$

with an uncertainty of at most 0.001 in the exponent. The latter is equal, within the numerical uncertainty, to the Hausdorff dimension. In fact, the asymptotic exponent is exactly s_0. We sketch a proof, omitting some tedious details.

Let $N^{\Pi}_{n,j}(\epsilon)$ be the number of cells of size greater than ϵ in $\mathcal{D}_j(n)$, and let $N^{\mathcal{D}}_{n,j}(\eta)$ be the number of tiles of arbitrary level and diameter greater than η in $D_j(n)$. Since

$$\frac{|\Pi_i(n, k_1, \ldots, k_L)|}{|\mathcal{D}_j(n, k_1, \ldots, k_L)|} = \frac{|\Pi_i(n')|}{|\mathcal{D}_j(n')|}, \qquad n' = h(n, k_1, \ldots, k_L),$$

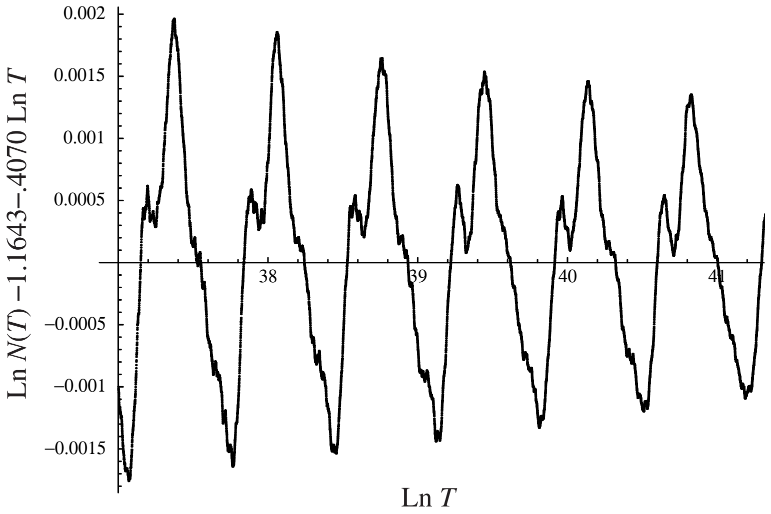

Figure 8: Fluctuations of $N(T)$ relative to the average power law (log-log plot).

the number of possible cell-tile diameter ratios is restricted to a finite set, labeled only by n', i, j. Moreover, the number of $\rho(n)$ images of $\Pi_i(n, k_1, \ldots, k_L)$ in $\mathcal{D}_j(n, k_1, \ldots, k_L)$ is identical to that of $\Pi_i(h(n, k_1, \ldots, k_L))$ in $\mathcal{D}_j(h(n, k_1, \ldots, k_L))$, and so these multiplicities are also limited to a finite number of possibilities. Thus it is easy to find positive, ϵ-independent real numbers $\gamma_\pm, \kappa_\pm$ such that

$$\gamma_- N^{\mathcal{D}}_{n,j}(\kappa_- \epsilon) < N^{\Pi}_{n,j}(\epsilon) < \gamma_+ N^{\mathcal{D}}_{n,j}(\kappa_+ \epsilon).$$

But upper and lower bounds for $N^{\mathcal{D}}_{n,j}(\eta)$ can be derived using the same mass distribution and inequalities employed in the proof of Theorem 4 (we omit details), giving positive, ϵ-independent bounds $B_\pm$ such that

$$B_- \epsilon^{-s_0} < N^{\Pi}_{n,j}(\epsilon) < B_+ \epsilon^{-s_0}.$$

This gives us the desired result for the exponent.

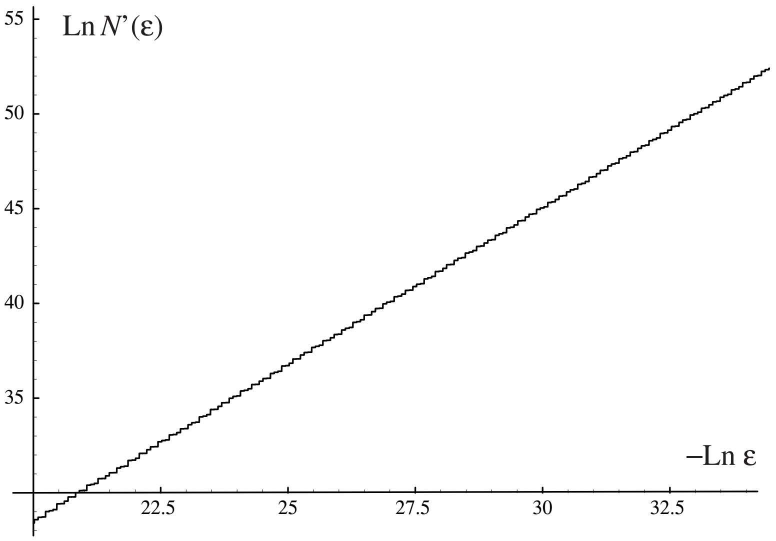

Figure 9: Log-log plot of the number of periodic cells with cell size greater than ϵ, as a function of ϵ.

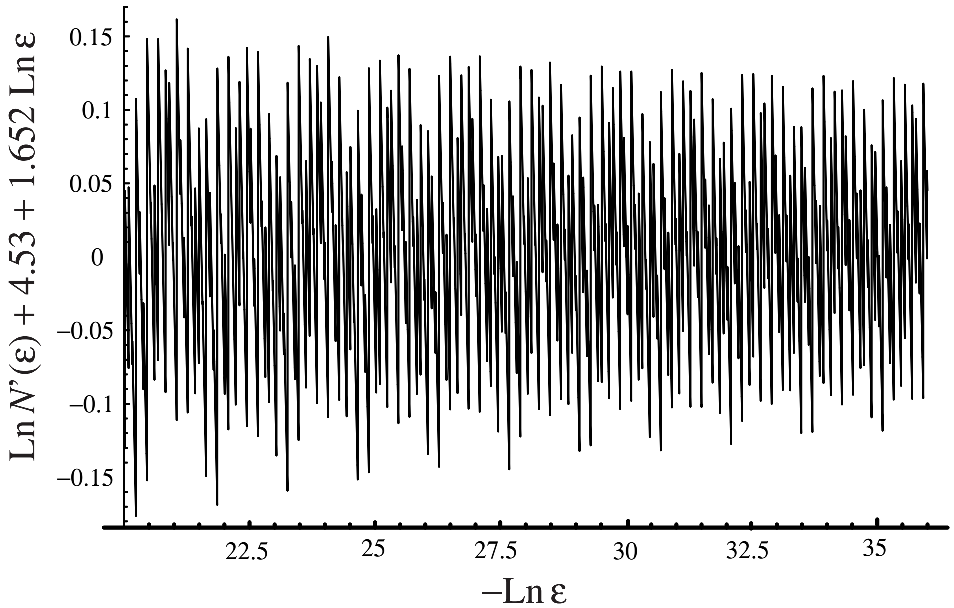

Figure 10: Fluctuations of $N'(\epsilon)$ relative to the average power law (log-log plot).

6 Tables

Domain	$\mathbf{m}$	Tiles	Sub-domains	Generating cells
$\Delta(0)$	$(7,2,11)$	$\mathcal{D}_0(0),\ldots,\mathcal{D}_2(0)$	$\Delta(0,0)\sim\Delta(1)$	$\Pi_0(0)$
$\Delta(1)$	$(7,1,11)$	$\mathcal{D}_0(1),\ldots,\mathcal{D}_{10}(1)$	$\Delta(1,0)\sim\Delta(2)$, $\Delta(1,1)\sim\Delta(1)$, $\Delta(1,2)\sim\Delta(1)$	$\Pi_0(1),\ldots,\Pi_8(1)$
$\Delta(2)$	$(7,1,9)$	$\mathcal{D}_0(2),\ldots,\mathcal{D}_{11}(2)$	$\Delta(2,0)\sim\Delta(2)$, $\Delta(2,1)\sim\Delta(1)$, $\Delta(2,2)\sim\Delta(1)$	$\Pi_0(2),\ldots,\Pi_5(2)$

Table 1: Catalogue of prototype dressed domains: $\Delta=\mathcal{D}((m_1,m_2,m_3),(1,1,1),(0,0,1))$ for Section 3.1.

Sub-domain	$\mathbf{m}$	b	ν	δ
$\mathcal{D}_0(0)$	$(3,11,7)$	$(-2-\lambda+\lambda^2,1,0)$	10	$(-2-\lambda+\lambda^2,-1)$
$\mathcal{D}_1(0)$	$(11,2,7)$	$(2+\lambda-\lambda^2,0,0)$	0	$(-1-\lambda+\lambda^2,-3+\lambda^2)$
$\mathcal{D}_2(0)$	$(4,2,10)$	$(-2-\lambda+\lambda^2,0,2+\lambda-\lambda^2)$	2	$(-1-\lambda+\lambda^2,2+\lambda-\lambda^2)$
$\mathcal{D}_0(1)$	$(3,1,11,7)$	$(-2-\lambda+\lambda^2,0,1,0)$	10	$(-2-\lambda+\lambda^2,-1)$
$\mathcal{D}_1(1)$	$(11,1,3,7)$	$(2+\lambda-\lambda^2,0,-5-\lambda+2\lambda^2,0)$	10	$(-5-\lambda+2\lambda^2,-2-\lambda+\lambda^2)$
$\mathcal{D}_2(1)$	$(10,13,1,5,7)$	$(5+\lambda-2\lambda^2,3-\lambda^2,0,-2+\lambda,0)$	12	$(-2+\lambda,3-\lambda^2)$
$\mathcal{D}_3(1)$	$(4,1,12,7)$	$(-3-2\lambda+2\lambda^2,0,2-\lambda,0)$	0	$(0,-2+\lambda)$
$\mathcal{D}_4(1)$	$(10,1,4,7)$	$(2+\lambda-\lambda^2,0,-2-\lambda+\lambda^2,-2+\lambda)$	0	$(-2+\lambda,0)$
$\mathcal{D}_5(1)$	$(10,6,4,0)$	$(2+\lambda-\lambda^2,2\lambda-\lambda^2,-2-\lambda+\lambda^2,2-\lambda)$	2	$(-1-\lambda+\lambda^2,2\lambda-\lambda^2)$
$\mathcal{D}_6(1)$	$(4,12,10)$	$(-2-\lambda+\lambda^2,7-2\lambda^2,2+\lambda-\lambda^2)$	0	$(3+2\lambda-2\lambda^2,3+2\lambda-2\lambda^2)$
$\mathcal{D}_7(1)$	$(10,6,1)$	$(5+\lambda-2\lambda^2,3-\lambda^2,0)$	8	$(0,-5-\lambda+2\lambda^2)$
$\mathcal{D}_8(1)$	$(3,1,11,7)$	$(-8-\lambda+3\lambda^2,0,3+2\lambda-2\lambda^2,0)$	10	$(-8-\lambda+3\lambda^2,-3-2\lambda+2\lambda^2)$
$\mathcal{D}_9(1)$	$(13,10,5)$	$(2\lambda-\lambda^2,2+\lambda-\lambda^2,-7+2\lambda^2)$	12	$(-7+2\lambda^2,-2\lambda+\lambda^2)$
$\mathcal{D}_{10}(1)$	$(1,10,7)$	$(0,8+\lambda-3\lambda^2,0)$	12	$(3+2\lambda-2\lambda^2,6+2\lambda-3\lambda^2)$
$\mathcal{D}_0(2)$	$(9,11,13,1,5,7)$	$(1,-\lambda+\lambda^2,1,0,1-\lambda,0)$	4	$(-\lambda+\lambda^2,-1+\lambda)$
$\mathcal{D}_1(2)$	$(4,9,0)$	$(\lambda-\lambda^2,1,1-2\lambda+\lambda^2)$	2	$(1,-1+3\lambda-\lambda^2)$
$\mathcal{D}_2(2)$	$(1,9,7)$	$(0,1,-1+2\lambda-\lambda^2)$	0	$(-1+2\lambda-\lambda^2,0)$
$\mathcal{D}_3(2)$	$(9,12,1,4,7)$	$(1-2\lambda+\lambda^2,-1+\lambda,0,-1+2\lambda-\lambda^2,0)$	0	$(2\lambda-\lambda^2,0)$
$\mathcal{D}_4(2)$	$(3,1,11,7)$	$(-2\lambda+\lambda^2,0,1-2\lambda+\lambda^2,0)$	2	$(1,2\lambda-\lambda^2)$
$\mathcal{D}_5(2)$	$(1,9,7)$	$(0,2-\lambda,0)$	0	$(-1+\lambda,0)$
$\mathcal{D}_6(2)$	$(2,12,7)$	$(-1+2\lambda-\lambda^2,-1+\lambda,0)$	12	$(1+\lambda-\lambda^2,1-\lambda)$
$\mathcal{D}_7(2)$	$(10,2,5,7)$	$(2\lambda-\lambda^2,-2+\lambda,3-\lambda^2,0)$	10	$(-1-\lambda+\lambda^2,1+\lambda-\lambda^2)$
$\mathcal{D}_8(2)$	$(1,11,7)$	$(0,-\lambda+\lambda^2,-2-\lambda+\lambda^2)$	6	$(-\lambda+\lambda^2,2+\lambda-\lambda^2)$
$\mathcal{D}_9(2)$	$(11,6,1)$	$(-\lambda+\lambda^2,-1,1+3\lambda-2\lambda^2)$	10	$(-2-3\lambda+2\lambda^2,1+4\lambda-3\lambda^2)$
$\mathcal{D}_{10}(2)$	$(8,6,0)$	$(-1-3\lambda+2\lambda^2,-1,2+\lambda-\lambda^2)$	12	$(3-4\lambda+\lambda^2,3\lambda-2\lambda^2)$
$\mathcal{D}_{11}(2)$	$(2,12,7)$	$(-2+\lambda,-3+\lambda^2,0)$	12	$(2+\lambda-\lambda^2,3-\lambda^2)$

Table 2: Domain map data for prototype dressed domains.

Sub-domain	κ	ν	δ	ω
$\Delta(0,0)$	0	10	$(-2-\lambda+\lambda^2,-1)$	1
$\Delta(1,0)$	0	3	$(2+\lambda-\lambda^2,2+\lambda-\lambda^2)$	$-2+3\lambda+4\lambda^2$
$\Delta(1,1)$	0	9	$(-11-3\lambda+5\lambda^2,-5-\lambda+2\lambda^2)$	$-2+3\lambda+4\lambda^2$
$\Delta(1,2)$	1	4	$(8+3\lambda-4\lambda^2,0)$	$-3+4\lambda+5\lambda^2$
$\Delta(2,0)$	0	0	$(0,0)$	$\lambda+\lambda^2$
$\Delta(2,1)$	1	7	$(1+\lambda-\lambda^2,1-\lambda)$	$-2+\lambda+2\lambda^2$
$\Delta(2,2)$	0	0	$(-2-\lambda+\lambda^2,0)$	$\lambda+\lambda^2$

Table 3: Dressed sub-domain data for prototype dressed domains.

Generating cell	ν	δ	ω	Multiplicities
$\Pi_0(0)$	0	$(6+2\lambda-3\lambda^2,0)$	$-4+6\lambda+7\lambda^2$	$(0,1,2)$
$\Pi_0(1)$	1	$(-9-2\lambda+4\lambda^2,-4-\lambda+2\lambda^2)$	$-2+3\lambda+3\lambda^2$	$(1,0,0,0,0,0,0,0,0,0,0)$
$\Pi_1(1)$	0	$(-30-14\lambda+17\lambda^2,-25-4\lambda+10\lambda^2)$	$-81+117\lambda+146\lambda^2$	$(48,0,3,10,10,6,0,0,0,0,0)$
$\Pi_2(1)$	1	$(-12-4\lambda+6\lambda^2,-6+2\lambda^2)$	$-9+13\lambda+16\lambda^2$	$(3,0,0,1,1,0,0,0,0,0,0)$
$\Pi_3(1)$	1	$(-20-5\lambda+9\lambda^2,-9-2\lambda+4\lambda^2)$	$-3+4\lambda+6\lambda^2$	$(0,1,0,0,0,0,0,0,0,0,0)$
$\Pi_4(1)$	1	$(42+11\lambda-19\lambda^2,-3+\lambda^2)$	$-65+94\lambda+117\lambda^2$	$(0,18,16,0,0,0,0,3,0,0,0)$
$\Pi_5(1)$	0	$(22+4\lambda-9\lambda^2,3+2\lambda-2\lambda^2)$	$-7+10\lambda+13\lambda^2$	$(0,0,1,0,0,0,0,0,0,0,0)$
$\Pi_6(1)$	0	$(28+6\lambda-12\lambda^2,3+2\lambda-2\lambda^2)$	$-36+52\lambda+65\lambda^2$	$(0,0,0,0,0,1,0,0,0,1,1)$
$\Pi_7(1)$	1	$(-31-8\lambda+14\lambda^2,-14-3\lambda+6\lambda^2)$	$-16+23\lambda+29\lambda^2$	$(0,0,0,0,0,0,0,0,1,0,0)$
$\Pi_8(1)$	1	$(-32-11\lambda+16\lambda^2,2\lambda-\lambda^2)$	$-81+117\lambda+146\lambda^2$	$(0,0,0,0,0,0,0,0,0,1,1)$
$\Pi_0(2)$	1	$(2+\lambda-\lambda^2,1)$	$-1+2\lambda+2\lambda^2$	$(1,0,0,0,0,0,0,0,0,0,0,0)$
$\Pi_1(2)$	0	$(16+9\lambda-10\lambda^2,7-2\lambda-\lambda^2)$	$-20+29\lambda+36\lambda^2$	$(3,0,0,0,0,0,0,0,0,1,2,0)$
$\Pi_2(2)$	1	$(-4-3\lambda+3\lambda^2,-3+4\lambda-\lambda^2)$	$-25+36\lambda+45\lambda^2$	$(0,16,0,7,6,0,3,0,0,0,0,0)$
$\Pi_3(2)$	0	$(-4+2\lambda,1-4\lambda+2\lambda^2)$	$-3+4\lambda+5\lambda^2$	$(0,1,0,1,0,0,0,0,0,0,0,0)$
$\Pi_4(2)$	0	$(-8-5\lambda+5\lambda^2,-5+\lambda+\lambda^2)$	$-25+36\lambda+45\lambda^2$	$(0,0,1,0,0,0,0,1,0,0,0,0)$
$\Pi_5(2)$	1	$(7-2\lambda-\lambda^2,2+3\lambda-2\lambda^2)$	$-11+16\lambda+20\lambda^2$	$(0,0,2,0,1,0,0,1,0,0,0,0)$

Table 4: Generating cells for prototype dressed domains.

Domain	$\mathbf{m}$	Tiles	Sub-domains	Generating cells
$\Delta(0)$	$(7,1,9)$	$\mathcal{D}_0(0),\ldots,\mathcal{D}_3(0)$	$\Delta(0,0)\sim\Delta(3),\Delta(0,1)\sim\Delta(1),\Delta(0,2)\sim\Delta(3)$	$\Pi_0(0),\ldots,\Pi_{27}(0)$
			$\Delta(0,3)\sim\Delta(1),\Delta(0,4)\sim\Delta(3),\Delta(0,5)\sim\Delta(1)$	
$\Delta(1)$	$(7,1,11)$	$\mathcal{D}_0(1),\ldots,\mathcal{D}_{10}(1)$	$\Delta(1,0)\sim\Delta(2),\ \Delta(1,1)\sim\Delta(1),\ \Delta(1,2)\sim\Delta(1)$	$\Pi_0(1),\ldots,\Pi_8(1)$
$\Delta(2)$	$(7,1,9)$	$\mathcal{D}_0(2),\ldots,\mathcal{D}_{11}(2)$	$\Delta(2,0)\sim\Delta(2),\Delta(2,1)\sim\Delta(1),\Delta(2,2)\sim\Delta(1)$	$\Pi_0(2),\ldots,\Pi_5(2)$
$\Delta(3)$	$(7,1,9)$	$\mathcal{D}_0(3),\ldots,\mathcal{D}_9(3)$	$\Delta(3,0)\sim\Delta(3),\ \Delta(3,1)\sim\Delta(1),\ \Delta(3,2)\sim\Delta(1)$	$\Pi_0(3),\ldots,\Pi_9(3)$

Table 5: Catalogue of prototype dressed domains $\Delta=\mathcal{D}((m_1,m_2,m_3),(1,1,1),(0,0,1))$ for Section 3.2.

$$A(0,0) = \begin{pmatrix} 1 & 1 & 1 & 1 & 1 & 1 & 1 & 1 & 1 & 1 & 1 \\ 0 & 1 & 2 & 2 & 2 & 2 & 2 & 4 & 2 & 2 & 2 \\ 0 & 0 & 1 & 2 & 2 & 3 & 2 & 6 & 0 & 1 & 1 \end{pmatrix}$$

$$A(1,0) = \begin{pmatrix} 0 & 3 & 0 & 0 & 0 & 0 & 0 & 0 & 0 & 0 & 0 & 0 \\ 0 & 0 & 0 & 0 & 0 & 0 & 0 & 0 & 0 & 0 & 0 & 0 \\ 0 & 0 & 0 & 0 & 0 & 0 & 0 & 0 & 0 & 0 & 0 & 0 \\ 0 & 2 & 1 & 0 & 0 & 0 & 0 & 0 & 0 & 0 & 0 & 0 \\ 0 & 2 & 1 & 0 & 0 & 0 & 0 & 0 & 0 & 0 & 0 & 0 \\ 2 & 0 & 0 & 2 & 1 & 0 & 3 & 0 & 4 & 10 & 9 & 0 \\ 1 & 1 & 1 & 1 & 1 & 1 & 1 & 1 & 1 & 1 & 1 & 1 \\ 0 & 0 & 0 & 0 & 0 & 0 & 0 & 0 & 0 & 0 & 0 & 0 \\ 0 & 0 & 0 & 0 & 0 & 0 & 0 & 0 & 3 & 6 & 6 & 0 \\ 0 & 0 & 0 & 1 & 0 & 0 & 2 & 1 & 1 & 7 & 6 & 4 \\ 0 & 0 & 0 & 1 & 0 & 0 & 2 & 1 & 1 & 7 & 6 & 4 \end{pmatrix} \qquad A(1,1) = \begin{pmatrix} 0 & 0 & 0 & 0 & 0 & 0 & 0 & 0 & 0 & 0 & 0 \\ 3 & 9 & 21 & 27 & 27 & 33 & 27 & 63 & 15 & 21 & 21 \\ 0 & 6 & 17 & 22 & 22 & 27 & 22 & 54 & 12 & 17 & 17 \\ 0 & 0 & 0 & 0 & 0 & 0 & 0 & 0 & 0 & 0 & 0 \\ 0 & 0 & 0 & 0 & 0 & 0 & 0 & 0 & 0 & 0 & 0 \\ 0 & 0 & 0 & 0 & 0 & 0 & 0 & 0 & 0 & 0 & 0 \\ 0 & 0 & 0 & 0 & 0 & 0 & 0 & 0 & 0 & 0 & 0 \\ 1 & 2 & 4 & 5 & 5 & 6 & 5 & 11 & 3 & 4 & 4 \\ 0 & 0 & 0 & 0 & 0 & 0 & 0 & 0 & 0 & 0 & 0 \\ 0 & 0 & 0 & 0 & 0 & 0 & 0 & 0 & 0 & 0 & 0 \\ 0 & 0 & 0 & 0 & 0 & 0 & 0 & 0 & 0 & 0 & 0 \end{pmatrix}$$

$$A(1,2) = \begin{pmatrix} 6 & 24 & 57 & 72 & 72 & 87 & 72 & 168 & 42 & 57 & 57 \\ 0 & 0 & 0 & 0 & 0 & 0 & 0 & 0 & 0 & 0 & 0 \\ 1 & 2 & 4 & 5 & 5 & 6 & 5 & 11 & 3 & 4 & 4 \\ 1 & 5 & 12 & 15 & 15 & 18 & 15 & 35 & 9 & 12 & 12 \\ 1 & 5 & 12 & 15 & 15 & 18 & 15 & 35 & 9 & 12 & 12 \\ 1 & 3 & 7 & 9 & 9 & 11 & 9 & 21 & 5 & 7 & 7 \\ 0 & 0 & 0 & 0 & 0 & 0 & 0 & 0 & 0 & 0 & 0 \\ 0 & 0 & 0 & 0 & 0 & 0 & 0 & 0 & 0 & 0 & 0 \\ 0 & 0 & 0 & 0 & 0 & 0 & 0 & 0 & 0 & 0 & 0 \\ 0 & 0 & 0 & 0 & 0 & 0 & 0 & 0 & 0 & 0 & 0 \\ 0 & 0 & 0 & 0 & 0 & 0 & 0 & 0 & 0 & 0 & 0 \end{pmatrix} \qquad A(2,0) = \begin{pmatrix} 0 & 0 & 0 & 0 & 0 & 0 & 0 & 0 & 0 & 0 & 0 & 0 \\ 0 & 1 & 0 & 0 & 0 & 0 & 0 & 0 & 0 & 0 & 0 & 0 \\ 3 & 2 & 2 & 4 & 2 & 1 & 6 & 2 & 6 & 18 & 16 & 5 \\ 0 & 2 & 1 & 0 & 0 & 0 & 0 & 0 & 0 & 0 & 0 & 0 \\ 2 & 0 & 0 & 2 & 1 & 0 & 3 & 0 & 4 & 10 & 9 & 0 \\ 1 & 1 & 1 & 1 & 1 & 1 & 1 & 1 & 1 & 1 & 1 & 1 \\ 0 & 0 & 0 & 0 & 0 & 0 & 0 & 0 & 0 & 0 & 0 & 0 \\ 0 & 0 & 0 & 1 & 0 & 0 & 2 & 1 & 0 & 5 & 4 & 4 \\ 0 & 0 & 0 & 0 & 0 & 0 & 0 & 0 & 0 & 0 & 0 & 0 \\ 0 & 0 & 0 & 0 & 0 & 0 & 0 & 0 & 0 & 0 & 0 & 0 \\ 0 & 0 & 0 & 0 & 0 & 0 & 0 & 0 & 0 & 0 & 0 & 0 \\ 0 & 0 & 0 & 0 & 0 & 0 & 0 & 0 & 1 & 2 & 2 & 0 \end{pmatrix}$$

$$A(2,1) = \begin{pmatrix} 0 & 0 & 0 & 0 & 0 & 0 & 0 & 0 & 0 & 0 & 0 \\ 2 & 8 & 19 & 24 & 24 & 29 & 24 & 56 & 14 & 19 & 19 \\ 0 & 0 & 0 & 0 & 0 & 0 & 0 & 0 & 0 & 0 & 0 \\ 0 & 3 & 8 & 10 & 10 & 12 & 10 & 24 & 6 & 8 & 8 \\ 1 & 3 & 7 & 9 & 9 & 11 & 9 & 21 & 5 & 7 & 7 \\ 0 & 0 & 0 & 0 & 0 & 0 & 0 & 0 & 0 & 0 & 0 \\ 1 & 2 & 4 & 5 & 5 & 6 & 5 & 11 & 3 & 4 & 4 \\ 0 & 0 & 0 & 0 & 0 & 0 & 0 & 0 & 0 & 0 & 0 \\ 0 & 0 & 0 & 0 & 0 & 0 & 0 & 0 & 0 & 0 & 0 \\ 0 & 0 & 0 & 0 & 0 & 0 & 0 & 0 & 0 & 0 & 0 \\ 0 & 0 & 0 & 0 & 0 & 0 & 0 & 0 & 0 & 0 & 0 \\ 0 & 0 & 0 & 0 & 0 & 0 & 0 & 0 & 0 & 0 & 0 \end{pmatrix} \qquad A(2,2) = \begin{pmatrix} 1 & 2 & 4 & 5 & 5 & 6 & 5 & 11 & 3 & 4 & 4 \\ 0 & 0 & 0 & 0 & 0 & 0 & 0 & 0 & 0 & 0 & 0 \\ 0 & 0 & 0 & 0 & 0 & 0 & 0 & 0 & 0 & 0 & 0 \\ 0 & 0 & 0 & 0 & 0 & 0 & 0 & 0 & 0 & 0 & 0 \\ 0 & 0 & 0 & 0 & 0 & 0 & 0 & 0 & 0 & 0 & 0 \\ 0 & 0 & 0 & 0 & 0 & 0 & 0 & 0 & 0 & 0 & 0 \\ 0 & 0 & 0 & 0 & 0 & 0 & 0 & 0 & 0 & 0 & 0 \\ 0 & 0 & 0 & 0 & 0 & 0 & 0 & 0 & 0 & 0 & 0 \\ 1 & 1 & 1 & 1 & 1 & 1 & 1 & 1 & 1 & 1 & 1 \\ 0 & 1 & 2 & 2 & 2 & 2 & 2 & 4 & 2 & 2 & 2 \\ 0 & 0 & 1 & 2 & 2 & 3 & 2 & 6 & 0 & 1 & 1 \\ 0 & 0 & 0 & 0 & 0 & 0 & 0 & 0 & 0 & 0 & 0 \end{pmatrix}$$

Table 6: Tiling matrices for prototype dressed domains.

References

[1] R. Adler, B. Kitchens and C. Tresser, Dynamics of nonergodic piecewise affine maps of the torus, *Ergod. Th. and Dynam. Sys.* **21** (2001) 959–999.

[2] D. A. Marcus, *Number fields*, Springer-Verlag, New York, (1977).

[3] P. Ashwin, Elliptic behaviour in the sawtooth standard map, *Phys. Lett. A* **232** (1997) 409–416.

[4] P. Ashwin, W. Chambers, and G. Petrov, Lossless digital filters overflow oscillations: approximations of invariant fractals, *Inter. J. Bifur. Chaos*, **7** (1997) 2603–2610.

[5] M. D. Boshernitzan and C. R. Carroll, An extension of Lagrange's theorem to interval exchange transformations over quadratic fields, *Journal d'Analyse Mathématique* **72** (1997) 21–44.

[6] P. Boyland, Dual billiards, twist maps and impact oscillators, *Nonlinearity* **9** (1996) 1411–1438.

[7] H. Bruin, A. Lambert, G. Poggiaspalla, S. Vaienti, Numerical Investigations of a Discontinuous Rotation of the Torus, *Chaos* **13** (2003) 558–571.

[8] J. Buzzi, Piecewise isometries have zero topological entropy, Dynamics of nonergodic piecewise affine maps of the torus, *Ergod. Th. and Dynam. Sys.* **21** (2001) 1371–1377.

[9] L. O. Chua and T. Lin, Chaos in digital filters, *IEEE Trans. Circuits and Systems,* **CAS-35** (1988) 648–658.

[10] L. O. Chua and T. Lin, Chaos and fractals from third order digital filters, *Int. J. Cir. Theor. Appl.* **18** (1990) 241–255.

[11] L. O. Chua and T. Lin, Fractal pattern of second order non-linear digital filters: a new symbolic analysis, *Int. J. Cir. Theor. Appl.* **18** (1990) 541–550.

[12] H. Cohen, *A course in computational algebraic number theory*, Springer-Verlag, New York, (1996).

[13] A. C. Davies, Nonlinear oscillations and chaos from digital filters overflow, *Phil. Trans. R. Soc. Lond.* **A 353** (1995) 85–99.

[14] K. J. Falconer, *Fractal geometry*, Wiley, New York (1990).

[15] A. Goetz, *Dynamics of piecewise isometries*, PhD Thesis, University of Chicago (1996).

[16] A. Goetz, Dynamics of a piecewise rotation, *Continuous and Discrete Dyn. Sys.,* **4** (1998) 593–608.

[17] A. Goetz, A self-similar example of a piecewise isometric attractor, Dynamical Systems (Luminy-Marseille, 1998), 248-258, World Sci. Publishing, River Edge, 2000.

[18] A. Goetz, Perturbation of 8-attractor and births of satellite systems, *Int. J. Bifurcation and Chaos* **8** (1999) 1485–1501.

[19] A. Goetz, Sofic subshifts and piecewise isometric systems, *Ergod. Theor. & Dyn. Sys.* **19** (1999) 1485–1501.

[20] A. Goetz, Dynamics of piecewise isometries, *Illinois Journal of Mathematics* **44** (2000) 465–478.

[21] A. Goetz, Stability of cells in non-hyperbolic piecewise affine maps and piecewise rotations, *Nonlinearity* **14** (2001) 205–219.

[22] A. Goetz and G. Poggiaspalla, Rotation by $\pi/7$, preprint (2002).

[23] E. Gutkin and N. Simanyi, Dual polygonal billiards and necklage dynamics, *Comm. Math. Phys* **143** (1992) 431–449.

[24] E. Gutkin and N. Haydn, Topological entropy of polygon exchange transformations and polygonal billiards, *Ergod. Th. and Dyn. Sys.* **17** (1997) 849–867.

[25] J. E. Hutchinson, Fractals and self-similarities, *Indiana University Journal of Mathematics* **30** (1981) 713–747.

[26] B. Kahng, Dynamics of symplectic affine maps on tori, PhD Thesis, University of Illinois at Urbana-Champain (2000).

[27] B. Kahng, Dynamics of symplectic piecewise affine elliptic rotation maps on tori, *Ergodic Theory and Dynamical Systems* **22** (2002) 483–505.

[28] B. Kahng, Dynamics of Kaleidoscopic Maps, Preprint (2002). (To appear in *Advances in Mathematics.*)

[29] K. L. Kouptsov, J.H. Lowenstein and F. Vivaldi, Quadratic rational rotations of the torus and dual lattice maps, *Nonlinearity*, **15** (2002) 1795–1482.

[30] J. H. Lowenstein, Pseudochaos for piecewise rational rotations, preprint, New York University (2003).

[31] J. H. Lowenstein, S. Hatjispyros and F. Vivaldi, Quasi-periodicity, global stability and scaling in a model of Hamiltonian round-off, *Chaos* **7** (1997) 49–66.

[32] J. H. Lowenstein and F. Vivaldi, Anomalous transport in a model of hamiltonian round-off errors, *Nonlinearity* **11** (1998) 1321–1350.

[33] J. H. Lowenstein and F. Vivaldi, Embedding dynamics for round-off errors near a periodic orbit, *Chaos* (2000) 747-755.

[34] J. H. Lowenstein, K. L. Kouptsov, and F. Vivaldi, Recursive tiling and geometry of piecewise rotations by $\pi/7$: electronic supplement (2003) `http://home.nyu.edu/~jhl2/RecursiveTiling/ElectronicSupplement.pdf`.

[35] R. Daniel Mauldin and S. C. Williams, Hausdorff dimension in graph directed constructions, *Trans. Am. Math. Soc.* **309** (1988) 811–829.

[36] G. Poggiaspalla, Auto-similarités dans les systèmes isométriques par morceaux, PhD thesis, Université de la Méditerranée, Aix-Marseille II, (2003).

[37] S. Tabachnikov, Dual billiards, *Russian Math. Surveys*, **48** (1993) 81–109.

[38] S. Tabachnikov, On the dual billiard problem, *Adv. Math.*, **115** (1995) 221–249.

[39] S. Tabachnikov, Asymptotic dynamics on the dual billiard transformation, *J. Stat. Phys.* **83** (1996) 27–37.

[40] F. Vivaldi, Periodicity and transport from round-off errors, *Exp. Math.*, **3** (1994) 303–315.

[41] F. Vivaldi and A. V. Shaidenko, Global stability of a class of discontinuous dual billiards, *Commun. Math. Phys.*, **110** (1987) 625–640.

[42] C. W. Wu and L. O. Chua, Properties of admissible sequences in a second-order digital filter with overflow non-linearity, *Int. J. Cir. Theoer. Appl.* **21** (1993) 299–307.